

Research Article

Assessment of Sources and Pollution Level of Airborne Toxic Metals through Foliar Dust in an Urban Roadside Environment

Triratnesh Gajbhiye^{1),2)}, Tanzil Gaffar Malik¹⁾, Chang-Hee Kang⁴⁾, Ki-Hyun Kim^{3),*}, Sudhir Kumar Pandey^{1),*}

¹⁾Department of Botany, Guru Ghasidas Central University, Bilaspur C.G., 495009, India

²⁾Department of Botany, Govt. Shankar Sao Patel College Waraseoni, M.P., 481331, India

³⁾Department of Civil & Environmental Engineering, Hanyang University, Seoul 04763, Republic of Korea

⁴⁾Department of Chemistry, Jeju National University, 66 Jejudaehakno, Jeju 13557, Republic of Korea

***Co-Corresponding authors.**

Tel: +82-2-2220-2325 (K.-H. Kim)
 +91-7587194630 (S.K. Pandey)

E-mail: kkim61@hanyang.ac.kr

(K.-H. Kim)

skpbhu@gmail.com;

pandey.sudhir@ggu.ac.in

(S.K. Pandey)

Received: 8 October 2021

Revised: 23 December 2021

Accepted: 13 January 2022

ABSTRACT Concentrations of 19 elements (Al, Fe, Ca, K, Mg, Na, S, Ti, Ba, Sr, Zn, V, Cu, Mn, Cr, Pb, Ni, Co, and Cd) in foliar dust samples were determined from 6 different roadside locations of Bilaspur city (Chhattisgarh), India. Principal component analysis (PCA) indicated the significance of vehicular activities followed by sources such as firework events and other industrial/regional/transboundary sources in foliar dust in the area of study. Risk assessment of metal levels in foliar dust was performed using several indices based on the data collected from different sites. The geo-accumulation index (*I_{geo}*) analysis indicated foliar dust was moderately and extremely polluted with S and Cd, respectively, while practically unpolluted with most other elements (Al, Fe, Ca, K, Mg, Na, Ti, Ba, Sr, Zn, V, Cu, Mn, Cr, Pb, Ni, and Co). The values of pollution (*I_{POLL}*) index and contamination factor (CF) of Cd indicated a high pollution level. Comparable results were found for the ecological risk (*Erⁱ*) of Cd (above 320) with a very high *Erⁱ* at all sites. In addition, the overall *Erⁱ* index (*R_i*) of foliar dust at all sites was very high due to a greater Cd contribution.

KEY WORDS Metals, Phytomonitoring, Source apportionment, Contamination, Pollution indices

1. INTRODUCTION

Pollution levels in the urban environment can be assessed by analyzing the structure and metal concentration of suspended dust. The toxic metal pollution in urban environments arises from many sources such as atmospheric deposition (dry and wet), degradation of vehicular parts and fluids, emission of particulate matter (PM), biological load (fallen leaves from roadside plants containing deposited airborne toxic metals) and road surface paint degradation (middle of the road) (Gajbhiye *et al.*, 2019; Cheng *et al.*, 2011; Liu *et al.*, 2010). Pollution of the roadside environment is caused by the emission of PM from vehicular exhaust particles, lubricant oil residue, wear and tear of vehicle parts (break lining, plating etc.), fragmentation of tires, bushings and bearings, decomposition of batteries, cracking of bumpers, and engine exhaust (Bhandarkar, 2013). Therefore, vehicular activities are major sources of toxic metal emission in roadside environments and are mainly responsible for the

contamination of roadside dusts and soil in urban areas (Karbassi *et al.*, 2015). Toxic metals are released through vehicular exhaust and accumulated further *via* mixing with suspended dust.

However, several researchers used foliar dust to assess pollution levels in specific areas (Simon *et al.*, 2014; Ugo- lini *et al.*, 2013). Based on these results, in general, the source of dust metals was mainly due to anthropogenic factors (airborne sources such as vehicles and industry) (Gajbhiye *et al.*, 2016a, b). Because foliar dust also contains very fine PM (up to respirable suspended particulate matter (RSPM)), it can easily enter the human body (Kim *et al.*, 2017; Sgrigna *et al.*, 2015). Hence, the presence of toxic metals in ambient dust can be very hazardous for human health and the surrounding environment (Kim *et al.*, 2017). Qiu *et al.* (2009) studied S and several toxic metals including Pb, Cd, Cr, Cu, and Zn in foliar dust originated from power plants and industrial, commercial, and traffic areas in urban Huizhou (China). The statistical analysis of foliar metal data (Zn, Cu, V, Co, Pb, Cr, and Ni) showed toxic metals (Cr, Pb, and Co) were emitted from vehicular sources in Guangzhou, China (Zheng *et al.*, 2013). Mori *et al.* (2015) examined foliar dust to determine roadside air pollution and reported the presence of 21 metals in the ambient air of Pescia, Italy. Similarly, air contaminants (Pb, Zn, Mn, Ni, Fe, Ca, Ba, S, and Sr) in foliar dust were also investigated in an urban area of Debrecen, Hungary (Simon *et al.*, 2014).

In recent years, contamination levels and risks associated with toxic metals have attracted much attention and several methods are being used to evaluate those (Men *et al.*, 2018). For instance, geo accumulation index (*Igeo*), contamination factor (*CF*), and ecological risk (Er^i) factors are generally used to evaluate contamination levels (Karbassi *et al.*, 2008; Qingjie *et al.*, 2008). The sampling of roadside dust and soil are important methods for assessment of toxic metal pollution in roadside environments (Ghanavati *et al.*, 2019; Liu *et al.*, 2019; Jadoon *et al.*, 2018; Dehghani *et al.*, 2017). In recent years, road dust and roadside soils have been used to analyze ecological risk through derivation of different pollution indices based on toxic metals pollution in many cities such as based on road-dust in Urumqi City, China: Wei *et al.*, 2009; Ulsan, Korea: Duong and Lee, 2011; Shanghai, China: Zhang *et al.*, 2013; Baotou, China: Xu *et al.*, 2015; Rafsanja, Iran: Aminiyan *et al.*, 2018; Nsukk, Nigeria: Mama *et al.*, 2020 and road-soil in Qinghai- Tibet plateau: Yan *et al.*, 2013; Ahvaz City, Iran: Ghanavati *et al.*, 2019.

Some researchers also used sediments and sewage sludge to assess the contamination level (Kirat and Aydin, 2018; Wei *et al.*, 2016; Huang *et al.*, 2011). Although it can be a very useful medium, foliar dust has not been used to estimate the ecological risk posed by airborne toxic elements.

In the present study, airborne toxic metals in foliar dust on numerous plants growing naturally at different roadside locations of a subtropical region in the city of Bilaspur (C.G.), India were determined. To explore the basic characteristics of pollution occurring in the urban roadside environment, a variety of metals that bound with the foliar dust were measured from different plant species using inductively coupled plasma - optical emission spectrometry (ICP-OES). Based on concentration data from the different sites, risk assessment of airborne toxic metals was conducted using several key pollution indices (geo-accumulation index (*Igeo*), contamination factor (*CF*), ecological risk (Er^i) and Er^i index (*RI*). *Igeo* and *CF* are used to assess the contamination level of different metals in foliar dust by comparing their concentration in samples and geochemical background values. Er^i represents the toxicity of metals which accounts for both the toxic response and *CF*. In contrast, *RI* estimates the potential risk which is mainly based on the toxicity of metals at a particular site. Previously, these indices have been employed to assess the level of metal pollution in sediments, soil and road dust. In the present study, these indices were also used to evaluate the factors and processes affecting toxic metal pollution that occurs in the form of foliar dust.

MATERIALS AND METHODS

2.1 Study Sites

Bilaspur is the second largest city in the Chhattisgarh state of India. The city is administered by Municipal Corporation with a metropolitan population of 616,000 (Source: Bilaspur, India Metro Area Population, 2021). The geographical location of Bilaspur is 22°05'N 82°09' E/22°09'N 82°15'E with an average elevation of 262 m (860 ft) (Gajbhiye *et al.*, 2016c). The climate of the city is pleasant in winter and generally hot and humid in summer. The temperature varies approximately from 9°C to 45°C. The monsoon generally arrives in the second week of June and continues until September. Average annual rainfall in the city is 1,259 mm (Source: TBC, IGKV, Bilaspur). Random sewer projects and unplanned road-

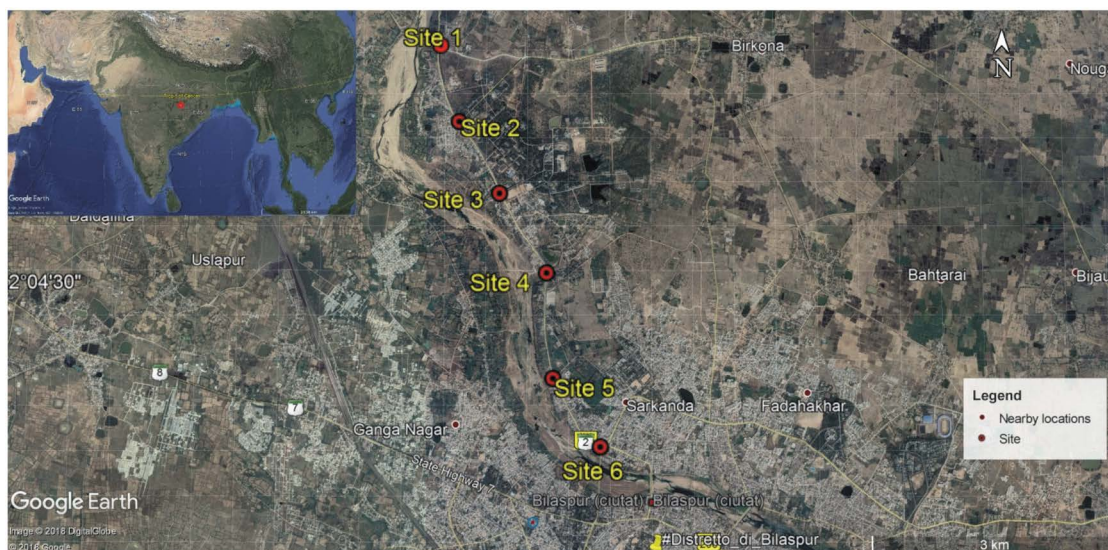


Fig. 1. Geographic locations of study sites in the city of Bilaspur (C.G.), India (Source = Google earth application-.kml/.kmz).

ways are responsible for regular traffic jams in the city. Big industrial areas (e.g. Sirgitti, Tifra and Silpahari) are located in and around Bilaspur. Moreover, large thermal power plants of the National Thermal Power Corporation (NTPC) and mining areas of South East Central Coalfields Limited (SECL) are located around the city.

In this study, 6 different roadside sites were selected for the collection of foliar dust. To this end, emphasis was given to represent diverse number and nature of traffic activities. (1) Turkadih Arpa Bridge near Koni: it is a bypass road which connects three national highways (NH 130 with NH 130A and NH 45). Most of the heavy vehicles passes through it with a reduced speed, (2) near Koni residential roadside area: it was affected by both heavy and light vehicular traffic which connect residential area to main road, (3) roadside in front of Guru Ghadas Central University, Bilaspur (GGU roadside) gate: affected by moderate vehicular activities; (4) Near the Bilasa Park Gate: on the road side affected by moderate vehicular activities, (5) Agricultural college gate: near to site 4, and (6) Seepat Chowk: a major traffic square in the city affected by heavy vehicle congestion and impacted by residential/commercial activities (Fig. 1).

2.2 Sampling

At each study site, plant species, especially trees/shrubs, were selected for the collection of dust depending on their availability, ease of sampling and height (Table S1). Consequently, a total of 35 dust samples were col-

lected from 6 different study sites: 4 from site 1 (*Annona squamosa*, *Calotropis procera*, *Citrus limon* and *Primula pulvereae*), 10 from site 2 (*Annona squamosa*, *Pongamia pinnata*, *Bambusa bambos*, *Butea monosperma*, *Capparis zeylanica*, *Ficus religiosa*, *Hemidesmus indicus*, *Alangium lamarckii*, *Senna siamea* and *Alstonia scholaris*), 11 from site 3 (*Ailanthus altissima*, *Alstonia scholaris*, *Antigonon leptopus Alba*, *Carissa carandas*, *Ficus benghalensis*, *Mitragyna parvifolia*, *Paulownia tomentosa*, *Ricinus communis*, *Saraca asoca*, *Alangium lamarckii* and *Senna siamea*), 5 from site 4 (*Artocarpus heterophyllus*, *Gmelina arborea*, *Psidium guajava*, *Senna siamea* and *Syzygium cumini*), 3 from site 5 (*Alstonia scholaris*, *Butea monosperma* and *Mitragyna parvifolia*) and 2 from site 6 (*Butea monosperma* and *Mangifera indica*). The foliar dust samples from each site were collected within 1 day to minimize temporal effects. This time represents the dry weather conditions near the end of the winter season. For foliar dust, leaf samples were collected at a height of around 1.5 m above ground level at all sites to match the ambient height and to minimize road dust re-suspension during sample collection. Three leaves (corresponding to three replicates) from each plant were collected at once toward the road side face in ziploc plastic bags and brought to the laboratory.

2.3 Sample Preparation

The leaves of individual plant were immersed in 100 mL of deionized water (using a 200-mL beaker) and

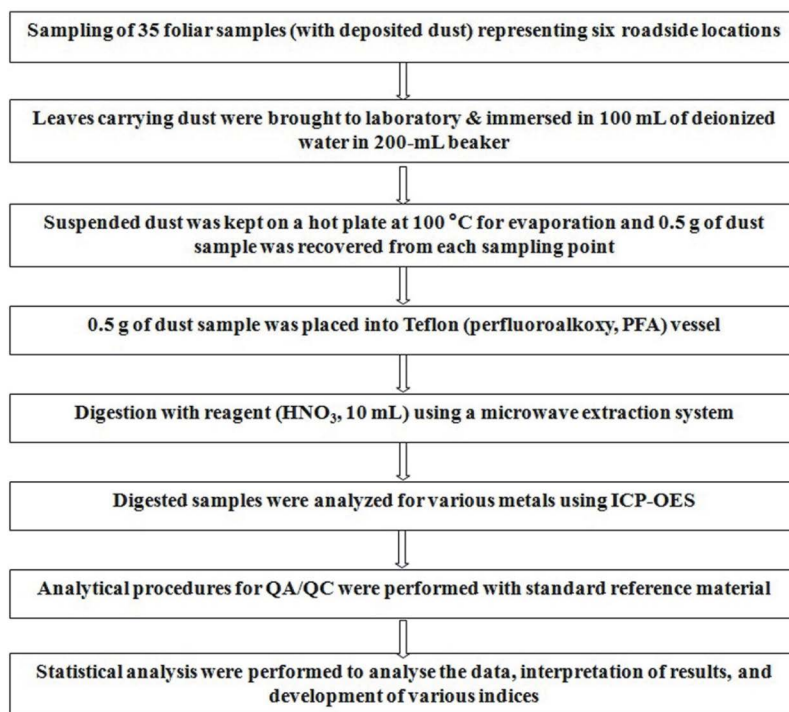


Fig. 2. A schematic diagram showing major steps of methodology in this study.

mixed firmly for five minutes. The water with the suspended dust was kept on a hot plate at 100°C for evaporation and recovery of the dust and 0.5 g of dust sample was separated for digestion. Sample preparation for the analysis of elemental species was performed using a microwave extraction system (Milestone, START D, USA) with nitric acid solution (US EPA Method 3051A) (Fig. 2). The dust samples were soaked in digestion reagent (HNO₃, 10 mL) in a Teflon (perfluoroalkoxy, PFA) vessel and digested under extreme pressure and temperature conditions conditions using the following procedures: (i) Temperature and pressure of the microwave digestion system were increased up to 180°C and 100 bar, respectively, for 10 min, with 1,000 W power; (ii) The temperature and pressure were steadily maintained for 15 min under above conditions with the same power; (iii) Teflon vessels were cooled down to reduce the temperature and pressure. Digestion vessels were cleaned by operating 2 blank runs using only 10 mL HNO₃ followed by washing with ultrapure water and finally drying with air. Extracted solutions were then transferred into a volumetric flask (25 mL volume) after filtration with Whatman PVDF syringe filter (0.45 µm) and the total volume was brought up to 25 mL with ultrapure water. As men-

tioned in method 3051A, it may not reflect the total metal content for certain metals (Al, Ba, Cr, Fe, Mg, and V: they require addition of HCl to be comparable with method 3050). Therefore, total mineralization methods with more aggressive acids (such as microwave-aqua-regia + HF) can also be used, however, with proper care, as it can also underestimate the concentration of metals such as Pb, Al, Ca, Fe, Mg, and Ba (Chen and Ma, 2001).

2.4 Quantification of Metals using ICP-OES

The sample solutions prepared using the above procedures were analyzed for various metals species using ICP-OES (Perkin Elmer, Model OPTIMA 7300DV, USA). The quality control of the analytical procedure was performed by analyzing standard reference material. The recovery analysis was conducted to evaluate the validity of the analytical procedure of various elemental species using certified reference material, CRM 1646a (Estuarine Sediment: National Institute of Standards and Technology, USA). The procedure and reagent used were the same as for the digestion and preparation of dust samples. The detection limit values achieved for target elements (expressed in µg mL⁻¹) were: Al (1.2), Fe (3.9), Ca (0.6), Na (1.6), K (3.9), Mg (1.5), Mn (0.3), Zn

(1.8), V (2.3), Cr (0.6), Pb (1.2), Cu (0.3), Ni (1.6), Co (0.7), S (7.8), and Cd (0.3). The repeatability was well below the 5% level for all the target elements, when expressed in terms of relative standard error (%) (e.g., 0.1% (Ca) to 4.4% (Ba)). The average recovery percentages obtained for available target species were determined and expressed in mean \pm RSD (relative standard deviation %) are as follows: Al ($44.6 \pm 9.4\%$), Fe ($88.8 \pm 3.8\%$), Ca ($99.6 \pm 2.5\%$), Na ($86.8 \pm 1.9\%$), K ($71.8 \pm 12.3\%$), Mg ($91.5 \pm 2.6\%$), Mn ($77.9 \pm 9.7\%$), Zn ($81.8 \pm 3.3\%$), V ($71.2 \pm 8.7\%$), Cr ($86.1 \pm 2.6\%$), Pb ($104.0 \pm 7.9\%$), Cu ($113.5 \pm 2.4\%$), Ni ($90.3 \pm 4.3\%$), Co ($91.8 \pm 2.8\%$), S ($96.5 \pm 9.9\%$), and Cd ($98.5 \pm 2.0\%$).

2.5 Statistical Analysis

The Normality of data were checked by a Shapiro-Wilk test and visual inspection of normal Q-Q plot through SPSS v16.0 (Razali and Wah, 2011). The summary statistics of this normality test is shown in the form of Table S2 and Fig. S1. As such, data were not normally distributed in most cases. As 19 metals of diverse nature were quantified in present study, it was important to identify their major sources. Principal component analysis (PCA) is frequently applied in environmental pollution research to assess relative information regarding pollution sources (Li *et al.*, 2017; Tang *et al.*, 2017). Moreover, PCA results in a considerable reduction in the number of variables and the detection of structure in the relationships of different variables. As such, PCA was applied using all the data of different metals measured at six sites as variables through XLSTAT 2018. The PCA was run based on the correlation matrix (Pearson (n)) type which standardized and scaled up the data. As there was not any missing data, do not accept missing data option was selected. For extraction of components, Eigen value (above 1), scree plot, and the total variance explained (above 70%) were considered. The bi-plots obtained were correlation bi-plots.

2.6 Assessment of Metal Pollution in Foliar Dust

2.6.1 *I_{geo}*

As the primary index, *I_{geo}* was first used to determine the metal pollution level in each dust sample (Müller, 1969) and was calculated according to equation (Eq. 1):

$$I_{geo} = \text{Log}_2(C_n/1.5B_n) \quad (1)$$

where C_n represents the measured concentration of ele-

ment n and B_n represents the background value of the element in fossil argillaceous samples (average shale). B_n was considered the concentration of metals in the earth's crust (Taylor and McLennan, 1995). The B_n values (mg/kg) of metals were 80,400 for Al, 35,000 for Fe, 30,000 for Ca, 28,000 for K, 13,300 for Mg, 260 for S, 28,900 for Na, 3,000 for Ti, 550 for Ba, 350 for Sr, 71 for Zn, 60 for V, 25 for Cu, 600 for Mn, 35 for Cr, 20 for Pb, 20 for Ni, 10 for Co and 0.098 for Cd (Taylor and McLennan, 1995; Taylor, 1964). As the background value of metals in the foliar dust was not assessed in this study, the background concentration values of metal in earth crust was considered to calculate the ecological risk index. The background matrix correction due to terrigenous effects was factor 1.5 to reduce the effects of potential variations in the control values and lithographic diversity (Lu *et al.*, 2009). The *I_{geo}* is classified as follows: $I_{geo} \leq 0$ (practically unpolluted), $0 < I_{geo} \leq 1$ (unpolluted to moderately polluted), $1 < I_{geo} \leq 2$ (moderately polluted), $2 < I_{geo} \leq 3$ (moderately to strongly polluted), $3 < I_{geo} \leq 4$ (strongly polluted), $4 < I_{geo} \leq 5$ (strongly to extremely polluted) and $I_{geo} > 5$ (extremely polluted). The above methodology adopted to estimate the *I_{geo}* considered mean metal concentrations in earth crust due to unavailability of soil metal data from the study area. However, consideration of the actual concentration of target metals in soil samples of study area at 100 cm depth will be more representative and realistic.

2.6.2 *I_{POLL}* Index

To assess the intensity of metal contamination in foliar dust, pollution index (*I_{POLL}*) was calculated according to Eq. 2 by Karbassi *et al.*, (2008):

$$I_{POLL} = \text{Log}_2(C_n/B_n) \quad (2)$$

C_n = metal concentration in foliar dust, B_n = geo-chemical concentration of metal in earth crust. The Müller *I_{geo}* equation was modified into *I_{POLL}* without correction factor (1.5) for calculating the intensity of metal contamination more precisely (Karbassi *et al.*, 2008). *I_{POLL}* is used to measure the effect of the metal pollution present in the lithosphere (Esmailzadeh *et al.*, 2016). *I_{POLL}* is classified according to *I_{geo}* categories.

2.6.3 *CF*

$$CF = C_n/B_n \quad (3)$$

The *CF* is the ratio between the concentrations of each metal in the samples and baseline or background value Eq.

3 (Hakanson, 1980). C_n is the measured concentration of metal in the sample and B_n is the geochemical background concentration of the metal (Taylor and McLennan, 1995). The level of pollution can be categorized based on CF values: $CF \leq 1$ low contamination, $1 \leq CF \leq 3$ moderate contamination and $CF \geq 3$ high contamination.

2.6.4 The Hakanson Potential RI Method

Er^i was proposed by Hakanson (1980) to quantitatively determine the potential Er^i of a given contaminant using the following Eq. 4:

$$Er^i = Tr \times CF \quad (4)$$

where Er^i is for a given substance, Tr represents the toxic response factor of a single element pollution ($Pb = Ni = Co = Cu = 5$, $Cr = V = 2$ (Xu *et al.*, 2015); $Ba = Zn = Mn = Ti = 1$ (Wei *et al.*, 2016; Zheng-Qi *et al.*, 2008); $Cd = 30$ (Hakanson, 1980) and CF represents the contamination factor. The Hakanson potential RI is thus calculated according to Eq. 5:

$$RI = \sum_1^n Er^i \quad (5)$$

where RI represents the potential for a given region/site. The pollution category of Er^i and RI values is given in Table S3.

3. RESULTS AND DISCUSSION

A total of 19 elements were detected in foliar dust samples. The concentrations of the elements determined from foliar dust are shown in Table 1.

3.1 Concentrations of Metals/Trace Elements at Different Sites

We quantified 19 elements (18 metals/transition metals/alkali metals/alkaline earth metals and 1 non-metal [S]) in foliar dust samples. Their concentrations ranged from 1.53 ± 0.37 mg/kg for Co to $177,728 \pm 32,793$ mg/kg for Fe. Subsequently, the metals were divided into 2 groups depending on their inclusion in hazardous air pollutant (HAP) listing: (i) metals/elements other than HAP list and (ii) metals in the US EPA HAP list.

3.1.1 Metals/Elements other than HAP List of EPA

As shown in Table 1a, when the general pattern was compared for each site, the metal concentrations at sites

1 showed the order of $Ca > Fe > Al > Mg > K > S > Na > Ti > Zn > Ba > Sr > V > Cu$, respectively. Moreover, site 2 and 4 also showed the similar pattern as $Ca > Fe > Mg > Al > K > S > Na > Ti > Zn > Ba > Sr > V > Cu$, respectively. At site 3, the order was changed mainly due to changes in K, S, Ba, and Zn. Moreover, at other sites (site 5 and 6) the pattern of $Fe > Mg > K > S > Ti > Ba$ was similar, however, changed for other elements. V and Cu showed the lowest concentration among all sites except site 6.

3.1.2 Metals in the US EPA HAP List (Mn, Cr, Ni, Co, Pb, and Cd)

As shown in Table 1c, the metal concentrations followed the order of $Mn > Cr > Pb > Ni > Cd > Co$ at site 1. The results obtained at sites 2, 3, and 4 followed the similar order of metal concentrations $Mn > Cr > Pb > Cd > Ni > Co$. At sites 4 and 6, the relative order was changed due to Pb, Cr, and Cd. In contrast, the Mn and Co showed maximum and minimum concentrations, respectively.

3.2 Comparison with Previous Studies

The mean concentrations of metals determined in this study were compared with concentrations reported in numerous previous studies from Calcutta, India (Chatterjee and Banerjee, 1999), Hangzhou, China (Lu *et al.*, 2008), Huizhou, China (Qiu *et al.*, 2009), Vienna, Austria (Simon *et al.*, 2011), Miskolc, Hungary (Simon *et al.*, 2016) and different locations in Bilaspur, India (Gajbhiye *et al.*, 2016a, c). The mean Al concentration (12,352 mg/kg) was more than 7 times higher than the Al concentration (1,683 mg/kg) in foliar dust of *P. acerifolia* leaf in Miskolc, Hungary. The mean Fe concentration (57,181 mg/kg) was more than 26 times higher than previously reported from other locations of Bilaspur, India (2,062 mg/kg) and Vienna, Austria (2,136 mg/kg) and 2 times higher than reported in Calcutta (21,800 mg/kg). The location of sites and traffic density is directly reflected on metal concentration in foliar dust (Zhang *et al.*, 2017). As such, in present study, significantly high vehicular activities compared to previous study might have contributed in significant deposition and enrichment of Fe in foliar dust. If we compare the concentration of metals across different sites in the present study, it reflects the influence of environmental factors such as traffic activity. For instance, as Site 6 was main traffic square of city with the highest traffic load, it showed the highest concentration

Table 1. Mean concentration of metals in foliar dust across different sites (unit = mg/kg, parameters = mean \pm SD (n)).

(a) Metals/elements other than HAP list							
Site	Al	Fe	Ca	K	Mg	S	Na
1	10093 \pm 3928 (4)	28839 \pm 5721 (4)	35145 \pm 7376 (4)	1666 \pm 869 (4)	7877 \pm 1476 (4)	1435 \pm 586 (4)	137 \pm 91 (4)
2	13126 \pm 3535 (10)	33035 \pm 6492 (10)	55154 \pm 19681 (10)	2625 \pm 604 (10)	13800 \pm 3900 (10)	1700 \pm 513 (10)	195 \pm 73 (10)
3	8062 \pm 2888 (11)	28262 \pm 9477 (11)	60158 \pm 23934 (11)	1499 \pm 381 (11)	15691 \pm 6636 (11)	1547 \pm 555 (11)	187 \pm 64 (11)
4	10319 \pm 1985 (5)	27979 \pm 5450 (5)	52317 \pm 8092 (5)	1904 \pm 380 (5)	12676 \pm 1718 (5)	1592 \pm 480 (5)	237 \pm 80 (5)
5	13539 \pm 4954 (3)	47243 \pm 22812 (3)	26109 \pm 8493 (3)	1906 \pm 863 (3)	6789 \pm 2047 (3)	1760 \pm 965 (3)	301 \pm 231 (3)
6	18971 \pm 794 (2)	177728 \pm 32793 (2)	2238 \pm 621 (2)	581 \pm 129 (2)	1010 \pm 54.1 (2)	518 \pm 10.9 (2)	46.5 \pm 13.1 (2)
Site	Ti	Ba	Sr	Zn	V	Cu	
1	121 \pm 73 (4)	35.1 \pm 10.0 (4)	34.8 \pm 9.47 (4)	44.1 \pm 30.3 (4)	18.5 \pm 2.70 (4)	11.5 \pm 4.76 (4)	
2	92.7 \pm 43 (10)	35.1 \pm 7.47 (10)	29.9 \pm 6.55 (10)	36.1 \pm 12.8 (10)	17.26 \pm 4.01 (10)	11.3 \pm 3.48 (10)	
3	35.7 \pm 12 (11)	29.8 \pm 6.67 (11)	28.9 \pm 5.84 (11)	18.1 \pm 5.04 (11)	9.48 \pm 3.60 (11)	7.98 \pm 2.49 (11)	
4	52.2 \pm 19.8 (5)	25.4 \pm 12.4 (5)	27.3 \pm 5.81 (5)	29.1 \pm 8.62 (5)	11.3 \pm 2.75 (5)	10.4 \pm 1.60 (5)	
5	53.5 \pm 25.8 (3)	29.7 \pm 7.81 (3)	16.8 \pm 9.48 (3)	20.4 \pm 10.9 (3)	14.9 \pm 1.49 (3)	9.83 \pm 1.20 (3)	
6	62.9 \pm 45.2 (2)	47.4 \pm 22.1 (2)	1.51 \pm 0.60 (2)	11.1 \pm 6.67 (2)	68.7 \pm 43.7 (2)	27.7 \pm 17.8 (2)	
(b) Metals on US EPA hazardous air pollutant (HAP) list							
Site	Mn	Cr	Pb	Ni	Co	Cd	
1	170 \pm 42 (4)	23.5 \pm 3.38 (4)	21.3 \pm 10.8 (4)	7.00 \pm 2.65 (4)	3.03 \pm 0.34 (4)	6.67 \pm 1.09 (4)	
2	142 \pm 32.7 (10)	21.10 \pm 4.61 (10)	17.4 \pm 3.82 (10)	4.79 \pm 1.09 (10)	2.40 \pm 0.68 (10)	6.77 \pm 1.52 (10)	
3	96.4 \pm 25.5 (11)	11.7 \pm 3.02 (11)	10.9 \pm 3.40 (11)	3.02 \pm 0.77 (11)	1.53 \pm 0.37 (11)	4.57 \pm 0.93 (11)	
4	114 \pm 29.8 (5)	13.2 \pm 3.34 (5)	14.1 \pm 3.29 (5)	3.65 \pm 0.91 (5)	1.81 \pm 0.36 (5)	5.11 \pm 0.95 (5)	
5	112 \pm 8.20 (3)	18.2 \pm 3.97 (3)	14.1 \pm 4.89 (3)	3.92 \pm 0.78 (3)	3.05 \pm 0.72 (3)	7.26 \pm 2.09 (3)	
6	195 \pm 126 (2)	61.7 \pm 39.1 (2)	26.4 \pm 16.9 (2)	7.34 \pm 4.21 (2)	5.45 \pm 2.93 (2)	29.1 \pm 10.8 (2)	

of metals (Al, Fe, Ba, V, Cu, Mn, Cr, Pb, Ni, Co, and Cd) in comparison to other sites (Table 1). The mean Ca concentration in the present study (38,520 mg/kg) was higher than in foliar dust in Vienna, Austria (29,427 mg/kg). However, mean K, Mg, and S concentrations were several times lower than in Vienna, Austria. Conversely, metals in the second group (Na, Ba, Sr, Zn, V, and Cu) showed comparably lower concentrations than previous studies. For example, the mean Na concentration (184 mg/kg) was more than 50 times lower than in Vienna, Austria. Similarly, mean Sr (23.2 mg/kg), Zn (26.5 mg/kg) and V (23.4 mg/kg) concentrations were approximately 4, 37, and 2 times lower than in Calcutta, India, respectively.

The mean concentration of metals (Mn, Cr, Pb, Ni, Co, and Cd) in the HAP category also showed highly variable patterns. The mean Mn level (138 mg/kg) in the present study was significantly lower than in previous studies. For example, Mn level was more than 2 times lower than in Bilaspur, India (392 mg/kg) and Miskolc, Hungary (364 mg/kg). In contrast, the mean Cr concentration (24.9 mg/kg) was nearly 2 times higher than in Bilaspur, India (15.2 mg/kg) and Miskolc, Hungary (12 mg/kg). Pb (17.4 mg/kg) was slightly lower than in Bilaspur (21.3 mg/kg) and Vienna, Austria (18 mg/kg). The mean Ni concentration (4.95 mg/kg) was 7 times lower than in Calcutta (38 mg/kg). If we compare the concentration of metal sin HAP category across different sites, it reflects the influence of variable source activities (mainly traffic activity). For instance, Site 6 showed the highest concentration of HAP metals (Pb, Ni, Cr, Mn, Co, and Cd) similar to other metals among all the sites (Table 1). Moreover, the micrometeorological conditions can also affect the concentrations of these metals up to a certain degree.

3.3 Sources Apportionment and Factors Affecting the Distribution of Metals

If the Eigen values above 1 is considered, there were four principal components extracted (Table S4). However, as shown in the scree plot, the cumulative variance explained by two principle components were 71.8% (Fig. 3), only two principle components (PC1 and PC2) were considered. As shown in Table 2, PC1 was dominated by Cr, Co, V, Cu, Cd, Pb, Mn, Fe, Al, Ti, and Ba explaining 48.8% of total variance. The presence of metals such as Cr, Co, Cu, Cd, Mn, and Pb and with high factor loadings/correlations of 0.962, 0.945, 0.896, 0.893, 0.880, and 0.856, respectively in PC1 indicated their likely ori-

Table 2. The results of principle component analyses using all the data of metal concentrations measured from 6 study sites (Values in bold are larger in magnitude).

(a) Factor loadings/correlations between variables and factors		
Variables	PC1	PC2
Al	0.702	0.269
Fe	0.798	-0.486
Ca	-0.464	0.493
Na	-0.222	0.155
K	-0.003	0.800
Mg	-0.472	0.410
S	-0.185	0.680
Ti	0.540	0.689
Mn	0.880	0.379
Ba	0.752	0.338
Sr	-0.351	0.719
Zn	0.309	0.875
V	0.941	-0.227
Cr	0.962	-0.153
Pb	0.856	0.395
Cu	0.896	-0.065
Ni	0.855	0.364
Co	0.945	-0.096
Cd	0.893	-0.374
Eigen value	9.272	4.379
Variance explained (%)	48.801	23.046
Cumulative variance (%)	48.801	71.847
(b) Contribution of variables (%)		
Variables	PC1	PC2
Al	5.316	1.659
Fe	6.863	5.389
Ca	2.323	5.545
Na	0.534	0.548
K	0.000	14.607
Mg	2.400	3.833
S	0.367	10.572
Ti	3.140	10.854
Mn	8.346	3.286
Ba	6.094	2.606
Sr	1.330	11.804
Zn	1.028	17.497
V	9.555	1.172
Cr	9.991	0.536
Pb	7.908	3.567
Cu	8.666	0.097
Ni	7.893	3.024
Co	9.635	0.211
Cd	8.610	3.195

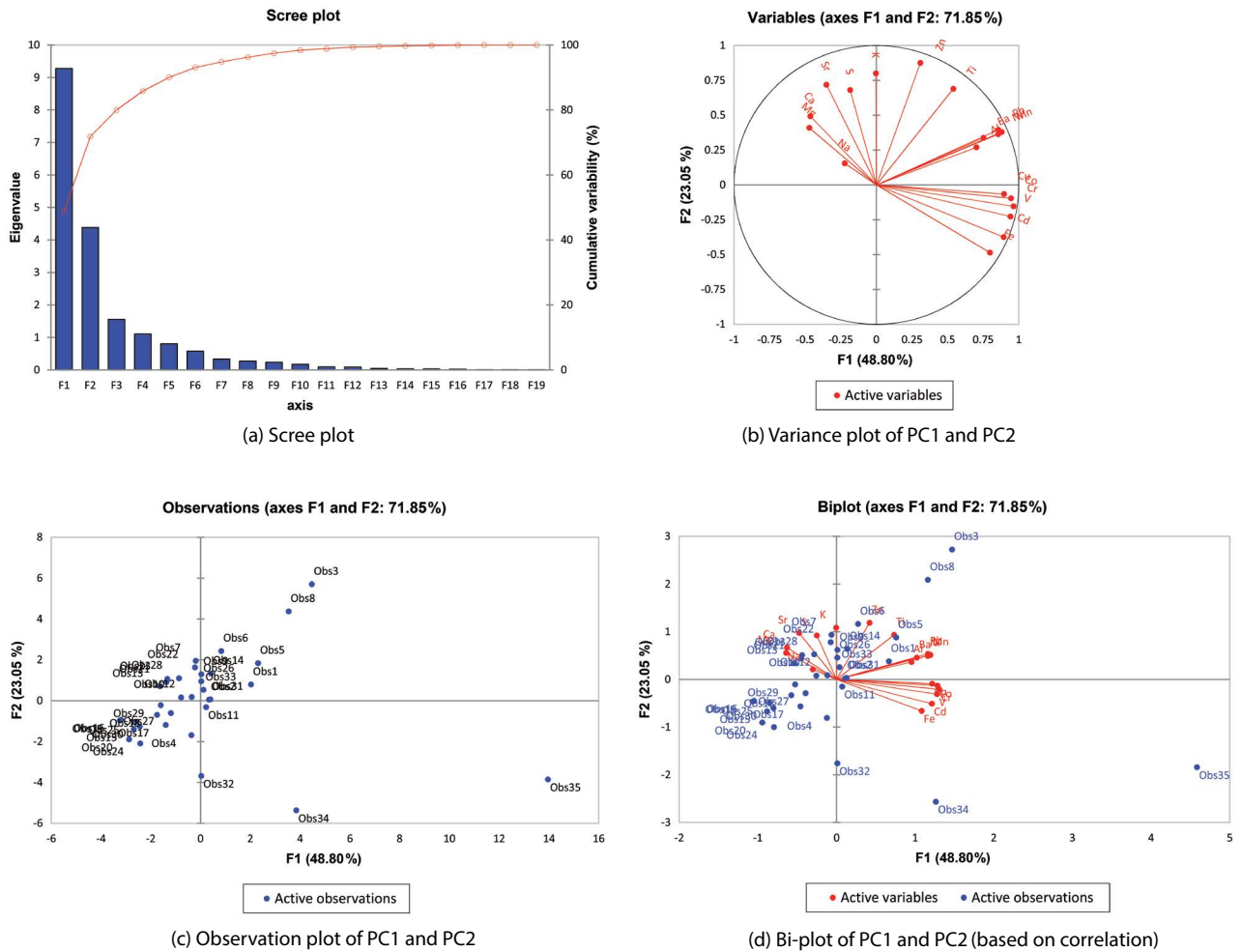


Fig. 3. The results of PCA in form of different plots considering all data of concentrations of 19 metals.

gin from corrosion in diesel/gasoline vehicles (braking, wearing of rust) use of fuel, lubricant, corrosion of metallic and engine parts, breakdown of vehicle tires and body parts, and vehicular exhaust (Gajbhiye *et al.*, 2019; Wu and Lu, 2018; Bourliva *et al.*, 2017; Li *et al.*, 2017). In the present study, all samples (foliar dust) were collected from the surface of leaves located near roadsides. Therefore, depending on the location of the sites and activities at the source, the primary source was apparently vehicular activities. The results of present study can be compared with previous studies conducted at sites affected by similar source characteristics. For instance, in present study, concentration of Cr (24.7 mg/kg) was considerably two times higher than previous studies such as Miskolc, Hungary (12 mg/kg) and Bilaspur, India (15.2 $\mu\text{g g}^{-1}$) (Gajbhiye, 2016a; Simon *et al.*, 2016). The mean Co concentration of present study was (2.88 mg/kg) nearly

3 orders of magnitude lower than those in Calcutta, India (9.73 mg/kg) and Guangzhou, China (8.09 mg/kg). However, it was relatively higher than those of Coimbatore, India (2.03 mg/kg) (Subpiramaniyam *et al.*, 2021; Liang *et al.*, 2019; Chatterjee and Banerjee, 1999). The mean concentration of Cu (13.1 mg/kg) in present study was much lower than those of Calcutta, India (269 mg/kg); Guangzhou, China (225 mg/kg); Outer-Ring Highway of Shanghai, China (191.8 mg/kg) (Liang *et al.*, 2019; Yin *et al.*, 2014; Chatterjee and Banerjee, 1999). The mean concentration of Cd (9.91 mg/kg) in foliar dust was around 4 time higher than those of Hangzhou, China (2.62 mg/kg) and Panzhihua, China (2.70 mg/kg) (Yang *et al.*, 2016; Lu *et al.*, 2008). In case of Pb, it was (17.4 mg/kg) 5 and 17 order of magnitude lower than those in Miskolc, Hungary (98 mg/kg) and Panzhihua, China (306.95 mg/kg), respectively (Simon *et al.*, 2016;

Yang *et al.*, 2016).

The PC2 showed 23.05 % of total variance with Zn, K, Sr, Ti, and S, as main contributors with a factor loading/correlation of 0.875, 0.800, 0.719, 0.689, and 0.680, respectively. There are a number of studies that reported a significant increase in elements such as Zn, Sr, Ti, K, and S in urban PM due to firework events (Dickerson *et al.*, 2017; Baranyai *et al.*, 2015). The study area covered in this study is also affected by significant firework events during several festivals throughout the year. Moreover, there is a usual practice of huge road processions in religious, political, and marriage events during which high amount of firework products are combusted for celebrations. As such, the high loadings of these metals in PC2 can be attributed to firework events at least in partial sense. However, when the mean concentration of metals of present study was compared with the metals emitted by fireworks events in previous studies, it was found that mean concentration of Sr (23.2 mg/kg) and Ti (69.7 mg/kg) was 20 and 600 order of magnitude higher than those of Coimbatore, India (Sr: 1.24 mg/kg; Ti: 0.10 mg/kg) (Subpiramaniyam *et al.*, 2021). In contrast, mean concentration of S (1,425 mg/kg) and K (1,697 mg/kg) was 6 and 12 order of magnitude lower than those of 9,417 mg/kg and 22,159 mg/kg south east part of Debrecen, Hungary, respectively (Baranyai *et al.*, 2015). Alternatively, mean concentration of Zn (26.5 mg/kg) was 12 orders of magnitude lower than those of Debrecen, Hungary (346 mg/kg) and Vienna, Austria (311 mg/kg) (Baranyai *et al.*, 2015; Simon *et al.*, 2011). Hence, it indicated that the factors other than vehicular activities such as firework events along with industrial (e.g., presence of power plants for sulfur emission)/commercial and/or regional/trans-boundary pollution could also potentially affect the distributions of metals at roadside locations in urban environment (Yadav *et al.*, 2018; Ismail *et al.*, 2017).

The foliar dust samples were collected from different plants growing near a given site. Thus, when the concentration of a given metal was compared across different plants at a given site, considerable variation was observed. Most toxic metals (e.g., metals listed as HAPs, such as Mn, Cr, Co, Ni, and Pb) showed the average variation in their concentration was 2-fold or less across different plants from different sites, except Cd where it was more than 4 times at site 6. The occurrence of significantly high level of Cd at site 6 is consistent with comparable concentrations found in foliar dust samples (23.5 to 34.3 mg/kg) near the same site in other study (Tiwari and Pandey,

2016). Site 6 (Seepat chowk) is a major traffic square of the city and adjacent to Nehru chowk where NH130A and NH 49 originate from NH 130 and connects Bilaspur City to other states of India. Hence, this site has significantly high traffic density and heavy vehicular load which might have contributed in the significantly high deposition and enrichment of Cd in foliar dust samples. It has been reported that traffic and industrial emissions were two main sources of Cd including with other HAP listed metals in suspended dust around road side environment (Hou *et al.*, 2019; Wang *et al.*, 2010). Emission of Cd results from the gasoline use, aging of automobile tires, car body wear, and brake lining wear (Weckwerth, 2001). Moreover, Cd can also possibly be emitted from paints used on the external surface of nearby public facilities (Li *et al.*, 2018). Moreover, the comparison of other metals (Al, Fe, Ca, Mg, and V) showed a more than 10-fold difference between their concentrations at site 3. Morphological variation in plant leaves has been reported to influence the retention and accumulation of dust on their surface (Gajbhiye *et al.*, 2019; Chen *et al.*, 2017). The deposition of foliar dust tends to remain temporary on leaf surfaces due to climatic conditions (rainfall, humidity, wind speed and direction, season, and temperature) (Schleicher *et al.*, 2011; Nowak *et al.*, 2006). Hence, the climatic conditions can also exert direct impacts on metal concentration through foliar dust.

3.4 Assessment of Pollution/Risk Level using Various Indices

3.4.1 Igeo

Toxic metal contaminants in foliar dust were assessed with *Igeo*. The *Igeo* was calculated for all metals at different sites (Table 3a). Based on the Müller *Igeo* index, all metals (Al, Fe, Ca, K, Mg, Na, Ti, Ba, Sr, Zn, V, Cu, Mn, Cr, Pb, Ni, and Co) showed values in the $Igeo \leq 0$ category (practically unpolluted) except S and Cd. The highest *Igeo* values were found for Cd at all sites ($Igeo > 5$), indicating extremely polluted conditions. Moreover, site 6 showed a maximum *Igeo* value (59.6) for Cd which represented a high traffic density square. The average *Igeo* for Cd (20.3) was approximately 20 times higher than road dust in Beijing, China (1.06; Tang *et al.*, 2013) and in Huainan, China (1.00; Tang *et al.*, 2017). The *Igeo* value for S ranged from 1.11 to 1.36 at sites 1 through 5, indicating a moderately polluted environment ($1 < Igeo \leq 2$). Similarly, the *Igeo* value for Fe (1.02) showed

Table 3. Various indices of metal pollution levels determined from foliar dust samples at different study sites

(a) Geo-accumulation index (I_{geo})																			
Site	Al	Fe	Ca	K	Mg	S	Na	Ti	Ba	Sr	Zn	V	Cu	Mn	Cr	Pb	Ni	Co	Cd
1	0.03	0.17	0.24	0.01	0.12	1.11	0.001	0.01	0.01	0.02	0.12	0.06	0.09	0.06	0.13	0.21	0.07	0.06	13.7
2	0.03	0.19	0.37	0.02	0.21	1.31	0.001	0.01	0.01	0.02	0.10	0.06	0.09	0.05	0.12	0.17	0.05	0.05	13.9
3	0.02	0.16	0.40	0.01	0.24	1.19	0.001	0.002	0.01	0.02	0.05	0.03	0.06	0.03	0.07	0.11	0.03	0.03	9.36
4	0.03	0.16	0.35	0.01	0.19	1.23	0.002	0.003	0.01	0.02	0.08	0.04	0.08	0.04	0.08	0.14	0.04	0.04	10.5
5	0.03	0.27	0.17	0.01	0.10	1.36	0.002	0.004	0.01	0.01	0.06	0.05	0.08	0.04	0.10	0.14	0.04	0.06	14.9
6	0.05	1.02	0.01	0.004	0.02	0.40	0.0003	0.004	0.02	0.001	0.03	0.23	0.22	0.07	0.35	0.26	0.07	0.11	59.6
(b) Pollution index (I_{POLL})																			
Site	Al	Fe	Ca	K	Mg	S	Na	Ti	Ba	Sr	Zn	V	Cu	Mn	Cr	Pb	Ni	Co	Cd
1	0.04	0.25	0.35	0.02	0.18	1.66	0.001	0.01	0.02	0.03	0.19	0.09	0.14	0.09	0.20	0.32	0.11	0.09	20.5
2	0.05	0.28	0.55	0.03	0.31	1.97	0.002	0.01	0.02	0.03	0.15	0.09	0.14	0.07	0.18	0.26	0.07	0.07	20.8
3	0.03	0.24	0.60	0.02	0.36	1.79	0.002	0.00	0.02	0.02	0.08	0.05	0.10	0.05	0.10	0.16	0.05	0.05	14.0
4	0.04	0.24	0.52	0.02	0.29	1.84	0.002	0.01	0.01	0.02	0.12	0.06	0.13	0.06	0.11	0.21	0.05	0.05	15.7
5	0.05	0.41	0.26	0.02	0.15	2.04	0.003	0.01	0.02	0.01	0.09	0.07	0.12	0.06	0.16	0.21	0.06	0.09	22.3
6	0.07	1.53	0.02	0.01	0.02	0.60	0.000	0.01	0.03	0.001	0.05	0.34	0.33	0.10	0.53	0.40	0.11	0.16	89.4
Average	0.05	0.49	0.39	0.02	0.22	1.65	0.002	0.01	0.02	0.02	0.11	0.12	0.16	0.07	0.21	0.26	0.07	0.09	30.4
(c) Contamination factor (CF)																			
Site	Al	Fe	Ca	K	Mg	S	Na	Ti	Ba	Sr	Zn	V	Cu	Mn	Cr	Pb	Ni	Co	Cd
1	0.13	0.82	1.17	0.06	0.59	5.52	0.005	0.04	0.06	0.10	0.62	0.31	0.46	0.28	0.67	1.07	0.35	0.30	68.1
2	0.16	0.94	1.84	0.09	1.04	6.54	0.01	0.03	0.06	0.09	0.51	0.29	0.45	0.24	0.60	0.87	0.24	0.24	69.1
3	0.10	0.81	2.01	0.05	1.18	5.95	0.01	0.01	0.05	0.08	0.25	0.16	0.32	0.16	0.33	0.55	0.15	0.15	46.6
4	0.13	0.80	1.74	0.07	0.95	6.12	0.01	0.02	0.05	0.08	0.41	0.19	0.42	0.19	0.38	0.71	0.18	0.18	52.1
5	0.17	1.35	0.87	0.07	0.51	6.77	0.01	0.02	0.05	0.05	0.29	0.25	0.39	0.19	0.52	0.71	0.20	0.31	74.1
6	0.24	5.08	0.07	0.02	0.08	1.99	0.00	0.02	0.09	0.00	0.16	1.15	1.11	0.33	1.76	1.32	0.37	0.55	297
(d) The potential ecological risk (Er^i) factors and risk index (RI) of toxic metals.																			
Site	Er^i											RI							
	Ti	Ba	Zn	V	Cu	Mn	Cr	Pb	Ni	Co	Cd								
1	0.04	0.06	0.62	0.62	2.30	0.28	1.34	5.33	1.75	1.52	2042	2056							
2	0.03	0.06	0.51	0.58	2.26	0.24	1.21	4.35	1.20	1.20	2072	2084							
3	0.01	0.05	0.25	0.32	1.60	0.16	0.67	2.73	0.76	0.77	1399	1406							
4	0.02	0.05	0.41	0.38	2.08	0.19	0.75	3.53	0.91	0.91	1564	1574							
5	0.02	0.05	0.29	0.50	1.97	0.19	1.04	3.53	0.98	1.53	2222	2233							
6	0.02	0.09	0.16	2.29	5.54	0.33	3.53	6.60	1.84	2.73	8908	8931							

moderate pollution only at site 6 ($1 < I_{geo} \leq 2$). Based on I_{geo} , the foliar dust of selected sites was mainly affected by Cd along with S. The I_{geo} values for these elements are mainly influenced by anthropogenic activity (traffic activity). The high I_{geo} for S can be correlated with SO_2 pollution in the area with many large thermal power plants.

3.4.2 I_{POLL} Index

The I_{POLL} index for Al, Fe, Ca, K, Mg, Na, Ti, Ba, Sr, Zn, V, Cu, Mn, Cr, Pb, Ni, and Co at all sites ranged from 0.001 to 0.60 and showed unpolluted to moderate pollution status (I_{POLL} below 1) except at site 6 (with an I_{POLL} of 1.53 for Fe showing moderate pollution status relative to other metals) (Table 3). However, I_{POLL} index for S (except site 6) was in moderately polluted category.

In present study, I_{POLL} of Cd in foliar dust was 30 times higher than those of Anzali Wetland sediments (0.92) and Hamedan soil samples (0.59) (Esmailzadeh *et al.*, 2016; Mohammadpour *et al.*, 2016) (Table 3). It reveals that foliar dust was extremely polluted in Cd.

3.4.3 CF

Based on the CF computations, a list of elements (Fe, Ca, Mg, V, Cu, Cr, Pb, and S) showed moderate contamination ($1 < CF \leq 3$) across different sites (Table 3). Regarding S, CF ranged from 1.99 (site 6) to 6.77 (site 5) with an average of 5.48, indicating a high level of S contamination ($CF \geq 3$). Fossil fuel emissions resulting from traffic activity, coal combustion residues and power plants can be considered as main sources of S in the form of SO₂ pollution in urban environments (Medunić *et al.*, 2016; Zhang *et al.*, 2012; Streets and Waldhow, 2000). In addition, the Cd CF ranged from 46.6 (site 3) to 297 (site 6) with an average of 101, corresponding to significantly high Cd contamination ($CF > 3$). These values were significantly higher than for Cd CF in the soil (12.99) in the Tiexi District of China (Sun *et al.*, 2010). In a previous study of Bilaspur, the enrichment factor of Cd in foliar dust ranged from 775 to 1,428 suggesting a strong source signature comparable to the present study (Gajbhiye *et al.*, 2016c).

3.4.4 Assessment of Potential Erⁱ of Metals in Foliar Dust

The concentration of metals in foliar dust is a serious concern for the maintenance of roadside environments (flora, fauna and human health). The Hakanson method provides a quantitative evaluation for the potential Erⁱ of different contaminant levels (Hakanson, 1980). This assessment method is a relatively rapid, simple and standard method to assess the degree of pollution caused by toxic metals as well as their adverse effects on the surrounding biological environment (Yan *et al.*, 2013). The Erⁱ factor and RI of 11 metals in foliar dust are summarized in Table 3d. All metals were in the category of low potential Erⁱ with an Erⁱ < 40 (Ti, Ba, Zn, Mn, V, Cu, Cr, Pb, Ni, and Co) except for Cd. However, the Erⁱ for Cd ranged from 1,399 (site 3) to 8,908 (site 6) with a mean value of 3,035 indicating significantly high Erⁱ at all sites. The mean value of Cd (Erⁱ) was 90 and 20 times higher than the reported values in Huainan, China (94.8: Tang *et al.*, 2017) and Xian, China, respectively (469: Li *et al.*, 2017). The RI denotes the sum of Erⁱ values for all met-

als at a site. RI values for all sites ranged from 1,406 to 8,931 indicating a significantly high Erⁱ. Most of the RI values were affected by a single toxic metal, Cd.

4. CONCLUSIONS

The concentrations of metals assessed in foliar dust samples of present study were significantly different across different plants showing differential retention capacities. Based on the results of present study, Cd and S were the most significant pollutants in foliar dust samples among all target species. Moreover, the concentration data for all metals when examined using different pollution indices indicated that most study sites were contaminated by toxic metals (especially Cd). This study also suggests that foliar dust can be used as feasible and cost effective medium to assess the presence of toxic metals in ambient air. Moreover, the results of risk assessment give direct indication towards the health risks which can be posed by PM bound toxic metals. Further research should be directed to assess the relative effect between different sources and mechanisms that control the transport, fate and behavior of these toxic metals in different matrices, especially living entities such as plants and animals.

ACKNOWLEDGEMENT

The first author is thankful for financial support to UGC, New Delhi, India for Rajiv Gandhi National Fellowship (RGNF). The corresponding author acknowledges the financial support from a UGC start-up grant, New Delhi, India (No.F. 20-1/2012(BSR)/20-2(3)/2012(BSR) and UGC-MRP grant (F. No.-43-311/2014 (SR)). This study was also supported by a grant from the National Research Foundation of Korea (NRF) funded by the Ministry of Science, ICT & Future Planning (No. 2016R1E1A1A01940995). All authors gratefully acknowledge the constructive criticism provided by three anonymous reviewers and the editor who immensely helped in improving the final version of this manuscript.

CONFLICTS OF INTEREST

On behalf of all authors, the corresponding author states that there is no conflict of interest.

REFERENCES

- Aminiyani, M.M., Baalousha, M., Mousavi, R., Aminiyani, F.M., Hosseini, H., Heydariyan, A. (2018) The ecological risk, source identification, and pollution assessment of heavy metals in road dust: a case study in Rafsanjan, SE Iran. *Environmental Science and Pollution Research*, 25(14), 13382–13395. <https://doi.org/10.1007/s11356-017-8539-y>
- Baranyai, E., Simon, E., Braun, M., Tóthmérész, B., Posta, J., Fábrián, I. (2015) The effect of a fireworks event on the amount and elemental concentration of deposited dust collected in the city of Debrecen, Hungary. *Air Quality, Atmosphere & Health*, 8(4), 359–365. <https://doi.org/10.1007/s11869-014-0290-7>
- Bhandarkar, S. (2013) Vehicular pollution, their effect on human health and mitigation measures. *Vehicle Engineering*, 1(2), 33–40.
- Bilaspur, India Metro Area Population 1950–2021. <https://www.macrotrends.net/cities/21204/bilaspur/population>
- Bourliva, A., Christophoridis, C., Papadopoulou, L., Giouri, K., Papadopoulos, A., Mitsika, E., Fytianos, K. (2017) Characterization, heavy metal content and health risk assessment of urban road dusts from the historic center of the city of Thessaloniki, Greece. *Environmental Geochemistry and Health*, 39(3), 611–634. <https://doi.org/10.1007/s10653-016-9836-y>
- Chatterjee, A., Banerjee, R.N. (1999) Determination of lead and other metals in a residential area of greater Calcutta. *Science of the Total Environment*, 227(2–3), 175–185. [https://doi.org/10.1016/S0048-9697\(99\)00026-1](https://doi.org/10.1016/S0048-9697(99)00026-1)
- Chen, L., Liu, C., Zhang, L., Zou, R., Zhang, Z. (2017) Variation in tree species ability to capture and retain airborne fine particulate matter (PM_{2.5}). *Scientific Reports*, 7(1), 1–11. <https://doi.org/10.1038/s41598-017-03360-1>
- Chen, M., Ma, L.Q. (2001) Comparison of three aqua regia digestion methods for twenty Florida soils. *Soil Science Society of America Journal*, 65(2), 491–499. <https://doi.org/10.2136/sssaj2001.652491x>
- Cheng, H., Ma, L., Zhao, C., Li, X., Wang, X., Liu, Y., Yang, K. (2011) Characterization of HCHs and DDTs in urban dust-fall and prediction of soil burden in a metropolis-Beijing, China. *Chemosphere*, 85(3), 406–411. <https://doi.org/10.1016/j.chemosphere.2011.07.066>
- Dehghani, S., Moore, F., Keshavarzi, B., Beverley, A.H. (2017) Health risk implications of potentially toxic metals in street dust and surface soil of Tehran, Iran. *Ecotoxicology and Environmental Safety*, 136, 92–103. <https://doi.org/10.1016/j.jcoenv.2016.10.037>
- Dickerson, A.S., Benson, A.F., Buckley, B., Chan, E.A. (2017) Concentrations of individual fine particulate matter components in the USA around July 4th. *Air Quality, Atmosphere & Health*, 10(3), 349–358. <https://doi.org/10.1007/s11869-016-0433-0>
- Duong, T.T., Lee, B.K. (2011) Determining contamination level of heavy metals in road dust from busy traffic areas with different characteristics. *Journal of Environmental Management*, 92(3), 554–562. <https://doi.org/10.1016/j.jenvman.2010.09.010>
- Esmailzadeh, M., Karbassi, A., Moattar, F. (2016) Assessment of metal pollution in the Anzali Wetland sediments using chemical partitioning method and pollution indices. *Acta Oceanologica Sinica*, 35(10), 28–36. <https://doi.org/10.1007/s13131-016-0920-z>
- Gajbhiye, T., Kim, K.H., Pandey, S.K., Brown, R.J. (2016a) Foliar transfer of dust and heavy metals on Roadside plants in a subtropical environment. *Asian Journal of Atmospheric Environment*, 10(3), 137–145. <https://doi.org/10.5572/ajae.2016.10.3.137>
- Gajbhiye, T., Pandey, S.K., Kim, K.H. (2016b) Factors controlling the deposition of airborne metals on plant leaves in a subtropical industrial environment. *Asian Journal of Atmospheric Environment*, 10(3), 162–167. <https://doi.org/10.5572/ajae.2016.10.3.162>
- Gajbhiye, T., Pandey, S.K., Kim, K.H., Szulejko, J.E., Prasad, S. (2016c) Airborne foliar transfer of PM bound heavy metals in *Cassia siamea*: a less common route of heavy metal accumulation. *Science of the Total Environment*, 573, 123–130. <https://doi.org/10.1016/j.jscitotenv.2016.08.099>
- Gajbhiye, T., Pandey, S.K., Lee, S.S., Kim, K.H. (2019) Size fractionated phytomonitoring of airborne particulate matter (PM) and speciation of PM bound toxic metals pollution through *Calotropis procera* in an urban environment. *Ecological Indicators*, 104, 32–40. <https://doi.org/10.1016/j.jecolind.2019.04.072>
- Ghanavati, N., Nazarpour, A., De Vivo, B. (2019) Ecological and human health risk assessment of toxic metals in street dusts and surface soils in Ahvaz, Iran. *Environmental Geochemistry and Health*, 41(2), 875–891. <https://doi.org/10.1007/s10653-018-0184-y>
- Hakanson, L. (1980) An ecological risk index for aquatic pollution control. A sedimentological approach. *Water Research*, 14(8), 975–1001. [https://doi.org/10.1016/0043-1354\(80\)90143-8](https://doi.org/10.1016/0043-1354(80)90143-8)
- Hou, S., Zheng, N., Tang, L., Ji, X., Li, Y., Hua, X. (2019) Pollution characteristics, sources, and health risk assessment of human exposure to Cu, Zn, Cd and Pb pollution in urban street dust across China between 2009 and 2018. *Environment International*, 128, 430–437. <https://doi.org/10.1016/j.envint.2019.04.046>
- Huang, H., Yuan, X., Zeng, G., Zhu, H., Li, H., Liu, Z., Jiang, H., Leng, L., Bi, W. (2011) Quantitative evaluation of heavy metals' pollution hazards in liquefaction residues of sewage sludge. *Bioresource Technology*, 102(22), 10346–10351. <https://doi.org/10.1016/j.biortech.2011.08.117>
- Jadoon, W.A., Khpalwak, W., Chidya, R.C.G., Abdel-Dayem, S.M.M.A., Takeda, K., Makhdoom, M.A., Sakugawa, H. (2018) Evaluation of levels, sources and health hazards of road-dust associated toxic metals in Jalalabad and Kabul Cities, Afghanistan. *Archives of Environmental Contamination and Toxicology*, 74(1), 32–45. <https://doi.org/10.1007/s00244-017-0475-9>
- Karbassi, A.R., Monavari, S.M., Bidhendi, G.R.N., Nouri, J., Nematpour, K. (2008) Metal pollution assessment of sediment and water in the Shur River. *Environmental Monitoring and Assessment*, 147(1), 107–116. <https://doi.org/10.1007/s10661-007-0102-8>

- Karbassi, A.R., Tajziehchi, S., Afshar, S. (2015) An investigation on heavy metals in soils around oil field area. *Global Journal of Environmental Science and Management*, 1(4), 275–282.
- Kim, K.H., Kumar, P., Szulejko, J.E., Adelodun, A.A., Junaid, M.F., Uchimiya, M., Chambers, S. (2017) Toward a better understanding of the impact of mass transit air pollutants on human health. *Chemosphere*, 174, 268–279. <https://doi.org/10.1016/j.chemosphere.2017.01.113>
- Kirat, G., Aydin, N. (2018) Investigation of metal pollution in Moryayla (Erzurum) and surrounding stream sediments, Turkey. *International Journal of Environmental Science and Technology*, 15(10), 2229–2240. <https://doi.org/10.1007/s13762-017-1611-9>
- Li, F., Jinxu, Y., Shao, L., Zhang, G., Wang, J., Jin, Z. (2018) Delineating the origin of Pb and Cd in the urban dust through elemental and stable isotopic ratio: a study from Hangzhou City, China. *Chemosphere*, 211, 674–683. <https://doi.org/10.1016/j.chemosphere.2018.07.199>
- Li, H.H., Chen, L.J., Yu, L., Guo, Z.B., Shan, C.Q., Lin, J.Q., Gu, Y.G., Yang, Z.B., Yang, Y.X., Shao, J.R., Zhu, X.M. (2017) Pollution characteristics and risk assessment of human exposure to oral bioaccessibility of heavy metals via urban street dusts from different functional areas in Chengdu, China. *Science of the Total Environment*, 586, 1076–1084. <https://doi.org/10.1016/j.scitotenv.2017.02.092>
- Liang, S.Y., Cui, J.L., Bi, X.Y., Luo, X.S., Li, X.D. (2019) Deciphering source contributions of trace metal contamination in urban soil, road dust, and foliar dust of Guangzhou, southern China. *Science of The Total Environment*, 695, 133596. <https://doi.org/10.1016/j.scitotenv.2019.133596>
- Liu, E., Wang, X., Liu, H., Liang, M., Zhu, Y., Li, Z. (2019) Chemical speciation, pollution and ecological risk of toxic metals in readily washed off road dust in a megacity (Nanjing), China. *Ecotoxicology and Environmental Safety*, 173, 381–392. <https://doi.org/10.1016/j.ecoenv.2019.02.019>
- Liu, Z., Zhang, Y., Li, L., Guo, R., Huang, K. (2010) Chemical Composition and Possible Sources of Elements in Dustfall in Pingdingshan City. In 2010 4th International Conference on Bioinformatics and Biomedical Engineering, IEEEE, 1–4. <https://doi.org/10.1109/ICBBE.2010.5516593>
- Lu, S.G., Zheng, Y.W., Bai, S.Q. (2008) A HRTEM/EDX approach to identification of the source of dust particles on urban tree leaves. *Atmospheric Environment*, 42(26), 6431–6441. <https://doi.org/10.1016/j.atmosenv.2008.04.039>
- Lu, X., Wang, L., Lei, K., Huang, J., Zhai, Y. (2009) Contamination assessment of copper, lead, zinc, manganese and nickel in street dust of Baoji, NW China. *Journal of Hazardous Materials*, 161(2–3), 1058–1062. <https://doi.org/10.1016/j.jhazmat.2008.04.052>
- Mama, C.N., Nnaji, C.C., Emenike, P.C., Chibueze, C.V. (2020) Potential environmental and human health risk of soil and roadside dust in a rapidly growing urban settlement. *International Journal of Environmental Science and Technology*, 17(4), 2385–2400. <https://doi.org/10.1007/s13762-020-02637-9>
- Medunić, G., Ahel, M., Mihalić, I.B., Srček, V.G., Kopjar, N., Fiket, Ž., Bituh, T., Mikac, I. (2016) Toxic airborne S, PAH, and trace element legacy of the superhigh-organic-sulphur Raša coal combustion: Cytotoxicity and genotoxicity assessment of soil and ash. *Science of the Total Environment*, 566, 306–319. <https://doi.org/10.1016/j.scitotenv.2016.05.096>
- Men, C., Liu, R., Xu, F., Wang, Q., Guo, L., Shen, Z. (2018) Pollution characteristics, risk assessment, and source apportionment of heavy metals in road dust in Beijing, China. *Science of the Total Environment*, 612, 138–147. <https://doi.org/10.1016/j.scitotenv.2017.08.123>
- Mohammadpour, G., Karbassi, A., Baghvand, A. (2016) Pollution intensity of nickel in agricultural soil of Hamedan region. *Caspian Journal of Environmental Sciences*, 14(1), 15–24.
- Mori, J., Sæbø, A., Hanslin, H.M., Teani, A., Ferrini, F., Fini, A., Burchi, G. (2015) Deposition of traffic-related air pollutants on leaves of six evergreen shrub species during a Mediterranean summer season. *Urban Forestry & Urban Greening*, 14(2), 264–273. <https://doi.org/10.1016/j.ufug.2015.02.008>
- Müller, G. (1969) Index of geoaccumulation in sediments of the Rhine River. *Geojournal*, 2, 108–118.
- Nowak, D.J., Crane, D.E., Stevens, J.C. (2006) Air pollution removal by urban trees and shrubs in the United States. *Urban Forestry & Urban Greening*, 4(3–4), 115–123. <https://doi.org/10.1016/j.ufug.2006.01.007>
- Qingjie, G., Jun, D., Yunchuan, X., Qingfei, W., Liqiang, Y. (2008) Calculating pollution indices by heavy metals in ecological geochemistry assessment and a case study in parks of Beijing. *Journal of China University of Geosciences*, 19(3), 230–241. [https://doi.org/10.1016/S1002-0705\(08\)60042-4](https://doi.org/10.1016/S1002-0705(08)60042-4)
- Qiu, Y., Guan, D., Song, W., Huang, K. (2009) Capture of heavy metals and sulfur by foliar dust in urban Huizhou, Guangdong Province, China. *Chemosphere*, 75(4), 447–452. <https://doi.org/10.1016/j.chemosphere.2008.12.061>
- Razali, N.M., Wah, Y.B. (2011) Power comparisons of shapiro-wilk, kolmogorov-smirnov, lilliefors and anderson-darling tests. *Journal of Statistical Modeling and Analytics*, 2(1), 21–33.
- Schleicher, N.J., Norra, S., Chai, F., Chen, Y., Wang, S., Cen, K., Yu, Y., Stüben, D. (2011) Temporal variability of trace metal mobility of urban particulate matter from Beijing - A contribution to health impact assessments of aerosols. *Atmospheric Environment*, 45(39), 7248–7265. <https://doi.org/10.1016/j.atmosenv.2011.08.067>
- Sgrigna, G., Sæbø, A., Gawronski, S., Popek, R., Calfapietra, C. (2015) Particulate Matter deposition on *Quercus ilex* leaves in an industrial city of central Italy. *Environmental Pollution*, 197, 187–194. <https://doi.org/10.1016/j.envpol.2014.11.030>
- Simon, E., Baranyai, E., Braun, M., Cserhádi, C., Fábíán, I., Tóthmérés, B. (2014) Elemental concentrations in deposited dust on leaves along an urbanization gradient. *Science of the Total Environment*, 490, 514–520. <https://doi.org/10.1016/j.scitotenv.2014.05.028>
- Simon, E., Braun, M., Vidic, A., Bogyó, D., Fábíán, I., Tóthmérés, B. (2011) Air pollution assessment based on elemental concentration of leaves tissue and foliage dust along an urbanization gradient in Vienna. *Environmental Pollution*

- tion, 159(5), 1229–1233. <https://doi.org/10.1016/j.envpol.2011.01.034>
- Simon, E., Harangi, S., Baranyai, E., Fábrián, I., Tóthmérész, B. (2016) Influence of past industry and urbanization on elemental concentrations in deposited dust and tree leaf tissue. *Urban Forestry & Urban Greening*, 20, 12–19. <https://doi.org/10.1016/j.ufug.2016.07.017>
- Streets, D.G., Waldhoff, S.T. (2000) Present and future emissions of air pollutants in China: SO₂, NO_x, and CO. *Atmospheric Environment*, 34(3), 363–374. [https://doi.org/10.1016/S1352-2310\(99\)00167-3](https://doi.org/10.1016/S1352-2310(99)00167-3)
- Subpiramaniyam, S., Boovaragamoorthy, G.M., Kaliannan, T., Krishna, K., Hong, S.C., Yi, P.L., Jang, S.H., Suh, J.M. (2021) Assessment of foliar dust deposition and elemental concentrations in foliar dust and long rows of grand tamarind leaves along two major roads of Coimbatore, India. *Chemosphere*, 264, 128444. <https://doi.org/10.1016/j.chemosphere.2020.128444>
- Sun, Y., Zhou, Q., Xie, X., Liu, R. (2010) Spatial, sources and risk assessment of heavy metal contamination of urban soils in typical regions of Shenyang, China. *Journal of Hazardous Materials*, 174(1–3), 455–462. <https://doi.org/10.1016/j.jhazmat.2009.09.074>
- Tang, R., Ma, K., Zhang, Y., Mao, Q. (2013) The spatial characteristics and pollution levels of metals in urban street dust of Beijing, China. *Applied Geochemistry*, 35, 88–98. <https://doi.org/10.1016/j.apgeochem.2013.03.016>
- Tang, Z., Chai, M., Cheng, J., Jin, J., Yang, Y., Nie, Z., Huang, Q., Li, Y. (2017) Contamination and health risks of heavy metals in street dust from a coal-mining city in eastern China. *Ecotoxicology and Environmental Safety*, 138, 83–91. <https://doi.org/10.1016/j.ecoenv.2016.11.003>
- Taylor, S.R. (1964) Abundance of chemical elements in the continental crust: a new table. *Geochimica et Cosmochimica Acta*, 28(8), 1273–1285. [https://doi.org/10.1016/0016-7037\(64\)90129-2](https://doi.org/10.1016/0016-7037(64)90129-2)
- Taylor, S.R., McLennan, S.M. (1995) The geochemical evolution of the continental crust. *Reviews of Geophysics*, 33(2), 241–265. <https://doi.org/10.1029/95RG00262>
- Tiwari, S., Pandey, S.K. (2016) Biomonitoring of toxic metals through roadside vegetation exposed to vehicular pollution in Bilaspur city. *Environmental Skeptics and Critics*, 5(3), 57.
- Ugolini, F., Tognetti, R., Raschi, A., Bacci, L. (2013) *Quercus ilex* L. as bioaccumulator for heavy metals in urban areas: effectiveness of leaf washing with distilled water and considerations on the trees distance from traffic. *Urban Forestry & Urban Greening*, 12(4), 576–584. <https://doi.org/10.1016/j.ufug.2013.05.007>
- US EPA (United States Environmental Protection Agency) Initial List of Hazardous Air Pollutants with Modifications include 187 hazardous air pollutants. Available at: <https://www.epa.gov/haps/initial-list-hazardous-air-pollutants-modifications>
- US EPA (United States Environmental Protection Agency) Method 3051A, Microwave assisted acid digestion of sediments, sludges, soils, and Oils. Available at: <https://www.epa.gov/sites/production/files/2015-12/documents/3051a.pdf>
- Wang, X., Huang, N., Dong, Z., Zhang, C. (2010) Mineral and trace element analysis in dustfall collected in the Hexi Corridor and its significance as an indicator of environmental changes. *Environmental Earth Sciences*, 60(1), 1–10. <https://doi.org/10.1007/s12665-009-0164-8>
- Weckwerth, G. (2001) Verification of traffic emitted aerosol components in the ambient air of Cologne (Germany). *Atmospheric Environment*, 35(32), 5525–5536. [https://doi.org/10.1016/S1352-2310\(01\)00234-5](https://doi.org/10.1016/S1352-2310(01)00234-5)
- Wei, B., Jiang, F., Li, X., Mu, S. (2009) Spatial distribution and contamination assessment of heavy metals in urban road dusts from Urumqi, NW China. *Microchemical Journal*, 93(2), 147–152. <https://doi.org/10.1016/j.microc.2009.06.001>
- Wei, X., Han, L., Gao, B., Zhou, H., Lu, J., Wan, X. (2016) Distribution, bioavailability, and potential risk assessment of the metals in tributary sediments of Three Gorges Reservoir: the impact of water impoundment. *Ecological Indicators*, 61, 667–675. <https://doi.org/10.1016/j.ecolind.2015.10.018>
- Wu, Y., Lu, X. (2018) Physicochemical properties and toxic elements in bus stop dusts from Qingyang, NW China. *Scientific Reports*, 8(1), 1–9. <https://doi.org/10.1038/s41598-018-30452-3>
- Xu, X., Lu, X., Han, X., Zhao, N. (2015) Ecological and health risk assessment of metal in resuspended particles of urban street dust from an industrial city in China. *Current Science*, 72–79.
- Yadav, S.K., Jain, M.K., Patel, D.K. (2018) Monitoring of Air Pollution in Different Regions Along Road Network, Jharia Coalfield, Dhanbad, India. In *Environmental pollution*, 125–134. Springer, Singapore. https://doi.org/10.1007/978-981-10-5792-2_10
- Yan, X., Gao, D., Zhang, F., Zeng, C., Xiang, W., Zhang, M. (2013) Relationships between heavy metal concentrations in roadside topsoil and distance to road edge based on field observations in the Qinghai-Tibet Plateau, China. *International Journal of Environmental Research and Public Health*, 10(3), 762–775. <https://doi.org/10.3390/ijerph10030762>
- Yang, J., Teng, Y., Song, L., Zuo, R. (2016) Tracing sources and contamination assessments of heavy metals in road and foliar dusts in a typical mining city, China. *PLoS One*, 11(12), e0168528. <https://doi.org/10.1371/journal.pone.0168528>
- Yin, R., Wang, D., Deng, H., Shi, R., Chen, Z. (2013) Heavy Metal Contamination and Assessment of Roadside and Foliar Dust along the Outer-Ring Highway of Shanghai, China. *Journal of Environmental Quality*, 42(6), 1724–1732. <https://doi.org/10.2134/jeq2013.04.0150>
- Zhang, J., Deng, H., Wang, D., Chen, Z., Xu, S. (2013) Toxic heavy metal contamination and risk assessment of street dust in small towns of Shanghai suburban area, China. *Environmental Science and Pollution Research*, 20(1), 323–332. <https://doi.org/10.1007/s11356-012-0908-y>
- Zhang, Q., He, K., Huo, H. (2012) Cleaning China's air. *Nature*, 484(7393), 161–162. <https://doi.org/10.1038/484161a>
- Zhang, T., Bai, Y., Hong, X., Sun, L., Liu, Y. (2017) Particulate matter and heavy metal deposition on the leaves of *Euonymus japonicus* during the East Asian monsoon in Beijing,

- China. PLoS One, 12(6), e0179840. <https://doi.org/10.1371/journal.pone.0179840>
- Zheng, Y., Gao, Q., Wen, X., Yang, M., Chen, H., Wu, Z., Lin, X. (2013) Multivariate statistical analysis of heavy metals in foliage dust near pedestrian bridges in Guangzhou, South China in 2009. *Environmental Earth Sciences*, 70(1), 107–113. <https://doi.org/10.1007/s12665-012-2107-z>
- Zheng-Qi, X., Shi-Jun, N., Xian-Guo, T., Cheng-Jiang, Z. (2008) Calculation of Heavy Metals' Toxicity Coefficient in the Evaluation of Potential Ecological Risk Index [J]. *Environmental Science & Technology*, 2(8), 31.

SUPPLEMENTARY MATERIALS

Table S1. Details of sampling sites for the analysis of metal concentrations in foliar dust and associated plant species.

Sites	Name of the plant species	GPS locations of study sites
Site 1	TURKADIH ARPA BRIDGE, KONI	N = 22°08'26.11"
1	<i>Annona squamosa</i>	E = 82°07'26.57"
2	<i>Calotropis procera</i>	
3	<i>Citrus limon</i>	
4	<i>Primula pulverea</i>	
Site 2	KONI, BILASPUR	N = 22°07'54.52"
1	<i>Annona squamosa</i>	E = 82°07'36.34"
2	<i>Pongamia pinnata</i>	
3	<i>Bambusa bambos</i>	
4	<i>Butea monosperma</i>	
5	<i>Capparis zeylanica</i>	
6	<i>Ficus religiose</i>	
7	<i>Hemidesmus indicus</i>	
8	<i>Alangium lamarckii</i>	
9	<i>Senna siamea</i>	
10	<i>Alstonia scholaris</i>	
Site 3	GGV ROAD SIDE	N = 22°07'25.22"
1	<i>Ailanthus altissima</i>	E = 82°07'54.31"
2	<i>Alstonia scholaris</i>	
3	<i>Antigonon leptopus Alba</i>	
4	<i>Carissa carandas</i>	
5	<i>Ficus benghalensis</i>	
6	<i>Mitragyna parvifolia</i>	
7	<i>Paulownia tomentosa</i>	
8	<i>Ricinus communis</i>	
9	<i>Saraca asoca</i>	
10	<i>Alangium lamarckii</i>	
11	<i>Senna siamea</i>	
Site 4	BILASA TAL	N = 22°06'52.96"
1	<i>Artocarpus heterophyllus</i>	E = 82°08'14.89"
2	<i>Gmelina arborea</i>	
3	<i>Psidium guajava</i>	
4	<i>Senna siamea</i>	
5	<i>Syzygium cumini</i>	
Site 5	AGRICULTURE COLLEGE GATE	N = 22°06'10.47"
1	<i>Alstonia scholaris</i>	E = 82°08'17.90"
2	<i>Butea monosperma</i>	
3	<i>Mitragyna parvifolia</i>	
Site 6	SEEPAT CHOWK	N = 22°05'43.38"
1	<i>Butea monosperma</i>	E = 82°08'38.11"
2	<i>Mangifera indica</i>	

Table S2. Details of summary statistics of Normality test based on Shapiro-Wilk test.

	Shapiro-Wilk		
	Statistic	df	Sig.
Al	.940	35	.055
Fe	.479	35	.000
Ca	.978	35	.693
Na	.856	35	.000
Mg	.980	35	.755
K	.979	35	.737
Ti	.831	35	.000
Ba	.938	35	.049
S	.972	35	.504
Zn	.836	35	.000
Cr	.586	35	.000
Sr	.909	35	.007
Pb	.823	35	.000
Ni	.810	35	.000
Co	.764	35	.000
V	.495	35	.000
Mn	.875	35	.001
Cd	.483	35	.000
Cu	.661	35	.000

Table S3. Relationships among ecological risk (Er^i) factors, risk index (RI) and pollution degree.

Er^i	Pollution degree	RI	Pollution degree
$Er^i < 40$	Low potential Er^i	$RI < 150$	Low Er^i
$40 \leq Er^i < 80$	Moderate potential Er^i	$150 \leq RI < 300$	Moderate Er^i
$80 \leq Er^i < 160$	Considerable potential Er^i	$300 \leq RI < 600$	Considerable Er^i
$160 \leq Er^i < 320$	High potential Er^i	$RI \geq 600$	Very high Er^i
$Er^i \geq 320$	Very high Er^i		

(Source = Yan *et al.*, 2013)

Table S4. The results of PCA considering all data of concentrations of 19 metals.

	Eigen value	Variability (%)	Cumulative (%)
F1	9.272	48.801	48.801
F2	4.379	23.046	71.847
F3	1.556	8.187	80.035
F4	1.102	5.800	85.835
F5	0.801	4.215	90.049
F6	0.576	3.033	93.082
F7	0.331	1.745	94.826
F8	0.272	1.429	96.256
F9	0.234	1.229	97.485
F10	0.171	0.902	98.387
F11	0.091	0.478	98.865
F12	0.087	0.459	99.325
F13	0.043	0.225	99.549
F14	0.030	0.157	99.707
F15	0.026	0.138	99.845
F16	0.021	0.110	99.955
F17	0.004	0.022	99.977
F18	0.003	0.013	99.991
F19	0.002	0.009	100.000

Table S5. Concentration of 19 metals measured across different sites and shown by plant species.

(a) Metals in high concentration range (above 500 mg/kg)							
Site	Plant species	Metals					
		Al	Fe	Ca	K	Mg	S
Site 1	<i>Annona squamosa</i>	9786.5	32857.4	34538.6	1610.4	7723.6	1346.0
	<i>Calotropis procera</i>	7609.8	23895.6	31715.9	1230.8	7548.4	1310.6
	<i>Citrus limon</i>	15738.0	34649.8	45617.2	2899.7	9892.1	2243.5
	<i>Primula pulverea</i>	7236.0	23954.9	28709.1	924.7	6345.7	841.7
Site 2	<i>Annona squamosa</i>	17885.6	32003.0	39055.4	2504.2	9972.4	1283.0
	<i>Pongamia pinnata</i>	14132.0	38453.7	91631.8	2141.6	20434.3	1675.0
	<i>Bambusa bambos</i>	15132.0	29353.7	51806.8	2727.8	13109.3	2965.0
	<i>Butea monosperma</i>	18814.0	42307.4	59063.6	3865.6	15791.1	1755.0
	<i>Capparis zeylanica</i>	13442.7	31021.6	49192.4	2980.4	11787.4	1763.3
	<i>Ficus religiose</i>	9699.0	20047.4	29238.6	2262.4	7376.1	1614.0
	<i>Hemidesmus indicus</i>	9938.0	30277.5	36579.5	2258.5	12631.2	1028.3
	<i>Alangium lamarckii</i>	10864.5	39478.7	57494.3	1686.6	18946.8	1600.0
	<i>Senna siamea</i>	8099.6	30053.0	83625.4	3065.2	14497.4	1420.0
	<i>Alstonia scholaris</i>	13257.0	37353.7	53856.8	2764.1	13459.3	1893.8
Site 3	<i>Ailanthus altissima</i>	7519.9	35383.2	68494.8	1274.7	17859.8	1012.5
	<i>Alstonia scholaris</i>	9643.5	34810.4	89811.6	1331.5	24489.7	1019.1
	<i>Antigonon leptopus Alba</i>	8199.5	26303.7	38469.3	1297.8	10661.8	1227.8
	<i>Carissa carandas</i>	10394.0	29555.4	59285.6	1873.9	13890.6	1300.8
	<i>Ficus benghalensis</i>	7681.5	31176.2	78452.3	1062.6	24873.9	1351.7
	<i>Mitragyna parvifolia</i>	1093.5	3192.0	5751.8	1514.4	1486.1	1878.7
	<i>Paulownia tomentosa</i>	11038.0	29285.8	72437.9	1894.4	16847.9	1960.0
	<i>Ricinus communis</i>	10715.6	38973.0	80135.4	1800.2	19907.4	1938.0
	<i>Saraca asoca</i>	9547.6	28653.0	67515.4	2064.2	15837.4	2842.0
	<i>Alangium lamarckii</i>	5198.3	22203.7	39956.8	842.2	10758.0	1150.8
	<i>Senna siamea</i>	7651.9	31341.0	61428.5	1535.7	15992.5	1330.3
	Site 4	<i>Artocarpus heterophyllus</i>	11014.3	30938.3	49359.1	1528.4	13040.7
<i>Gmelina arborea</i>		11198.0	30487.7	47266.1	2415.6	11644.3	1037.3
<i>Psidium guajava</i>		12396.3	33169.1	66187.9	2191.9	15222.9	2165.8
<i>Senna siamea</i>		7167.8	19486.5	52392.7	1729.6	12818.7	1308.0
<i>Syzygium cumini</i>		9816.4	25812.6	46378.1	1654.8	10652.2	1436.2
Site 5	<i>Alstonia scholaris</i>	10815.6	32503.0	29565.4	1702.2	7685.4	2426.0
	<i>Butea monosperma</i>	10544.5	73518.9	16433.1	1163.0	4447.1	653.2
	<i>Mitragyna parvifolia</i>	19257.1	35705.9	32329.7	2852.8	8235.2	2201.8
Site 6	<i>Butea monosperma</i>	18409.9	154539.8	2677.3	490.1	971.6	525.7
	<i>Mangifera indica</i>	19532.6	200916.4	1799.6	672.5	1048.2	510.2

Table S5. Continued.

(b) Metals in medium concentration range (below 500 mg/kg)								
Site	Plant species	Metals						
		Na	Ti	Cu	Ba	Sr	Zn	V
Site 1	<i>Annona squamosa</i>	94.5	99.8	9.5	36.9	31.3	36.6	19.0
	<i>Calotropis procera</i>	119.4	69.1	14.6	30.2	47.4	33.4	17.4
	<i>Citrus limon</i>	270.4	229.6	16.0	48.3	35.5	88.1	22.0
	<i>Primula pulverea</i>	65.6	86.4	5.7	25.1	25.0	18.5	15.7
Site 2	<i>Annona squamosa</i>	243.2	132.6	11.5	46.0	32.3	41.7	20.0
	<i>Pongamia pinnata</i>	149.9	89.9	12.4	41.3	44.8	40.4	21.0
	<i>Bambusa bambos</i>	173.7	104.4	8.0	34.0	26.0	38.7	16.3
	<i>Butea monosperma</i>	204.2	175.6	14.0	48.2	30.5	66.1	26.3
	<i>Capparis zeylanica</i>	143.6	99.2	8.3	31.3	23.7	37.0	15.5
	<i>Ficus religiose</i>	159.0	120.8	5.8	28.9	21.0	29.1	13.3
	<i>Hemidesmus indicus</i>	107.3	59.9	16.9	28.6	27.2	28.0	15.8
	<i>Alangium lamarckii</i>	189.0	49.4	12.9	32.2	29.8	27.4	15.4
	<i>Senna siamea</i>	373.1	36.8	9.0	26.7	34.2	17.7	13.5
	<i>Alstonia scholaris</i>	210.1	58.9	14.6	34.5	30.3	35.0	15.8
Site 3	<i>Ailanthus altissima</i>	188.0	30.3	6.7	24.9	26.1	13.4	9.2
	<i>Alstonia scholaris</i>	135.4	22.1	5.6	24.9	28.2	12.5	8.2
	<i>Antigonon leptopus Alba</i>	161.2	54.5	6.9	29.7	23.4	18.9	10.8
	<i>Carissa carandas</i>	197.3	35.4	9.0	29.5	25.6	19.6	10.5
	<i>Ficus benghalensis</i>	125.3	18.3	6.9	26.5	29.2	14.0	7.9
	<i>Mitragyna parvifolia</i>	144.4	33.8	6.3	24.8	26.7	15.9	0.8
	<i>Paulownia tomentosa</i>	211.1	49.5	9.1	40.0	35.9	25.4	11.5
	<i>Ricinus communis</i>	359.6	53.2	13.1	42.5	42.1	25.9	15.8
	<i>Saraca asoca</i>	188.5	32.6	11.8	36.0	31.4	24.3	11.3
	<i>Alangium lamarckii</i>	143.0	30.8	6.1	23.2	21.4	14.7	8.5
	<i>Senna siamea</i>	199.8	32.6	6.3	25.8	28.7	14.9	9.7
Site 4	<i>Artocarpus heterophyllus</i>	170.6	80.0	11.2	40.6	31.3	35.7	14.0
	<i>Gmelina arborea</i>	172.3	48.1	9.9	28.9	23.3	20.6	10.7
	<i>Psidium guajava</i>	255.6	63.9	12.4	6.6	34.8	33.7	14.3
	<i>Senna siamea</i>	221.5	37.9	10.6	28.6	26.3	36.6	9.2
	<i>Syzygium cumini</i>	365.0	31.2	8.1	22.4	20.6	18.9	8.3
Site 5	<i>Alstonia scholaris</i>	156.7	65.6	11.2	31.8	23.6	28.4	14.8
	<i>Butea monosperma</i>	566.6	23.9	8.9	21.1	6.0	8.0	16.5
	<i>Mitragyna parvifolia</i>	178.2	71.1	9.4	36.3	20.8	24.8	13.6
Site 6	<i>Butea monosperma</i>	37.3	30.9	15.1	31.8	1.1	6.4	37.8
	<i>Mangifera indica</i>	55.8	94.9	40.3	63.0	1.9	15.8	99.6

Table S5. Continued.

(c) Metals on US EPA hazardous air pollutant (HAP) list							
Site	Plant species	Metals					
		Cr	Pb	Mn	Ni	Co	Cd
Site 1	<i>Annona squamosa</i>	25.6	19.9	191.1	8.9	3.4	6.8
	<i>Calotropis procera</i>	19.2	17.4	137.1	4.7	3.0	7.8
	<i>Citrus limon</i>	26.7	36.7	218.2	9.7	3.2	7.0
	<i>Primula pulverea</i>	22.4	11.2	132.2	4.7	2.6	5.2
Site 2	<i>Annona squamosa</i>	25.2	15.9	171.8	6.8	3.5	8.1
	<i>Pongamia pinnata</i>	24.7	19.1	161.9	5.1	2.9	8.9
	<i>Bambusa bambos</i>	19.7	12.2	122.6	4.3	2.2	6.1
	<i>Butea monosperma</i>	31.1	25.4	214.9	6.6	3.4	9.0
	<i>Capparis zeylanica</i>	18.4	17.7	126.1	4.7	1.9	5.5
	<i>Ficus religiosa</i>	15.4	16.4	108.1	3.6	1.4	4.3
	<i>Hemidesmus indicus</i>	17.8	18.3	127.2	4.0	2.4	7.0
	<i>Alangium lamarckii</i>	20.4	14.8	136.8	3.9	2.3	6.6
	<i>Senna siamea</i>	19.3	13.2	110.1	4.4	1.8	5.8
	<i>Alstonia scholaris</i>	19.1	20.6	141.9	4.4	2.3	6.4
Site 3	<i>Ailanthus altissima</i>	9.9	8.6	83.9	2.5	1.4	4.5
	<i>Alstonia scholaris</i>	9.2	7.8	74.8	2.3	1.2	3.9
	<i>Antigonon leptopus</i> Alba	14.6	12.3	109.2	3.6	1.6	4.1
	<i>Carissa carandas</i>	12.1	10.5	90.9	3.1	1.6	5.1
	<i>Ficus benghalensis</i>	8.7	8.2	72.0	2.3	1.2	3.9
	<i>Mitragyna parvifolia</i>	8.5	7.6	75.1	2.3	1.2	4.1
	<i>Paulownia tomentosa</i>	13.3	12.5	114.0	3.5	1.8	4.9
	<i>Ricinus communis</i>	18.4	18.2	160.8	4.2	2.4	6.8
	<i>Saraca asoca</i>	13.3	15.1	100.4	4.3	1.7	4.7
	<i>Alangium lamarckii</i>	10.4	11.2	94.3	2.6	1.3	3.3
	<i>Senna siamea</i>	10.1	8.5	84.7	2.6	1.4	4.9
Site 4	<i>Artocarpus heterophyllus</i>	16.7	17.2	142.6	4.4	2.1	5.5
	<i>Gmelina arborea</i>	12.1	12.4	105.3	3.3	1.7	5.0
	<i>Psidium guajava</i>	16.5	17.2	145.8	4.7	2.3	6.5
	<i>Senna siamea</i>	11.4	13.9	101.6	3.4	1.7	4.5
	<i>Syzygium cumini</i>	9.2	9.5	75.4	2.4	1.4	4.0
Site 5	<i>Alstonia scholaris</i>	18.5	19.5	119.3	4.7	3.0	6.3
	<i>Butea monosperma</i>	21.9	10.1	103.1	3.2	3.8	9.7
	<i>Mitragyna parvifolia</i>	14.0	12.6	112.9	3.8	2.3	5.8
Site 6	<i>Butea monosperma</i>	34.0	14.5	105.8	4.4	3.4	21.5
	<i>Mangifera indica</i>	89.3	38.4	283.5	10.3	7.5	36.8

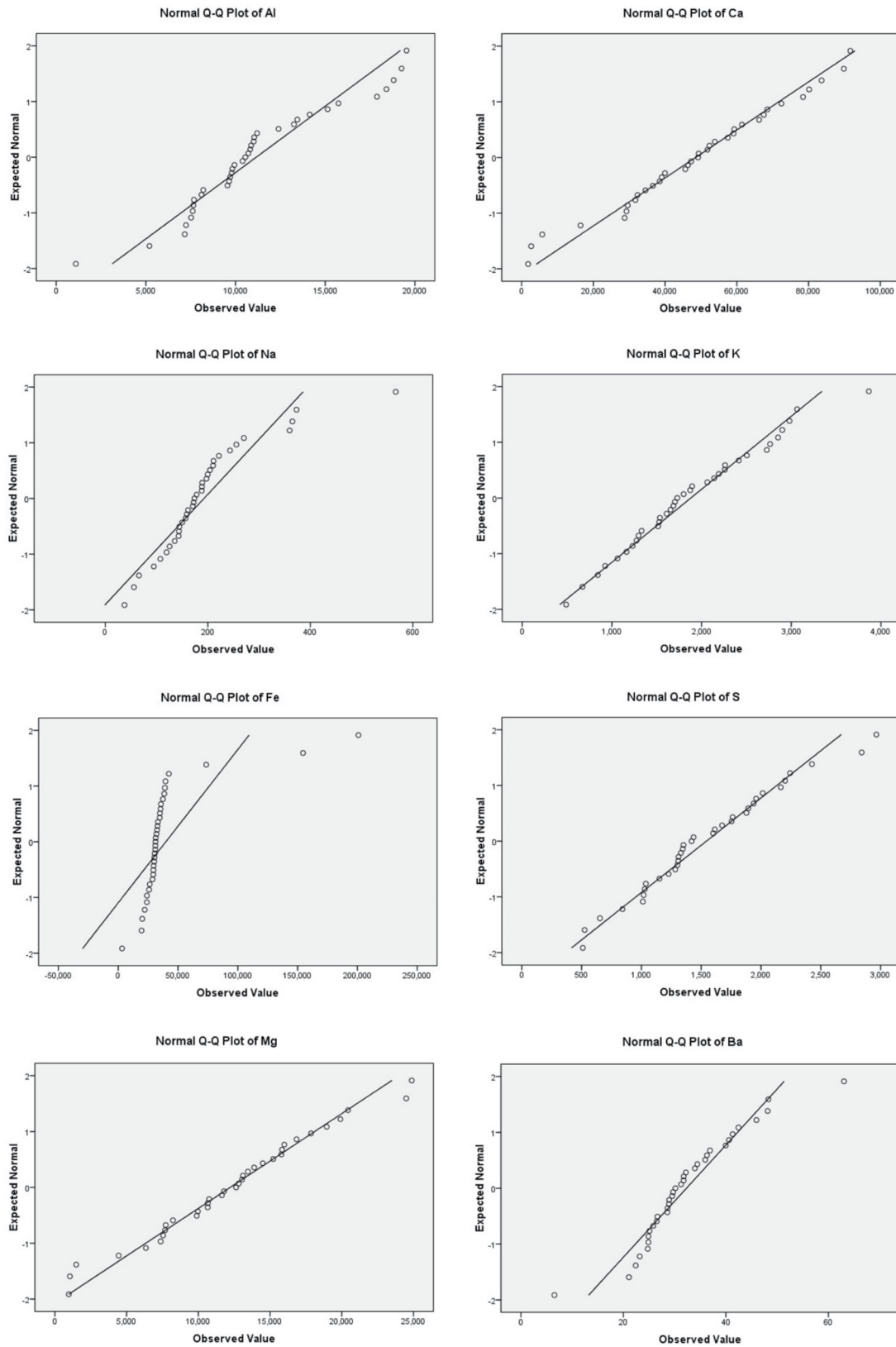


Fig. S1. Q-Q plots of 19 metals obtained through Shapiro-Wilk normality test.

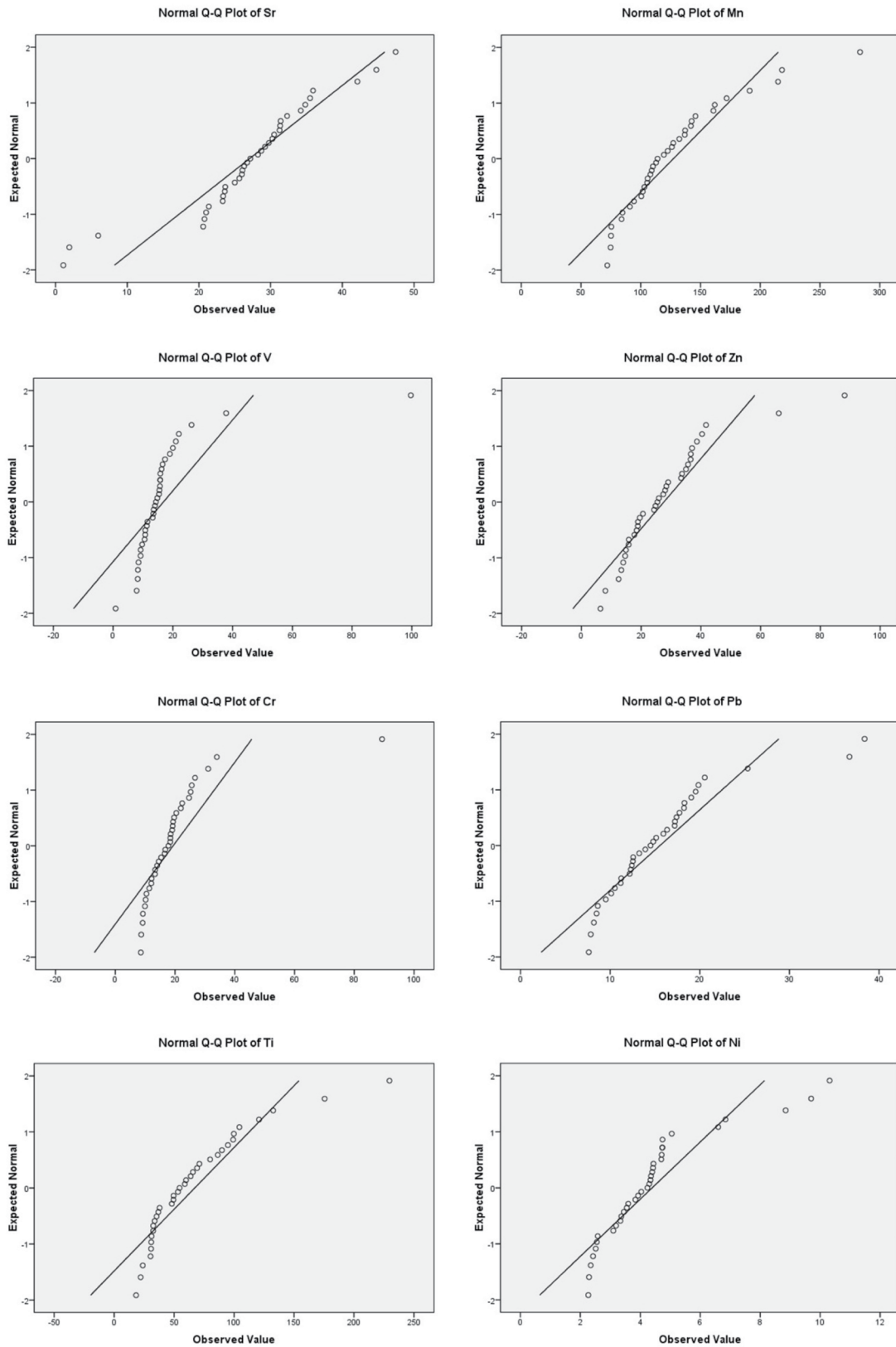


Fig. S1. Continued.

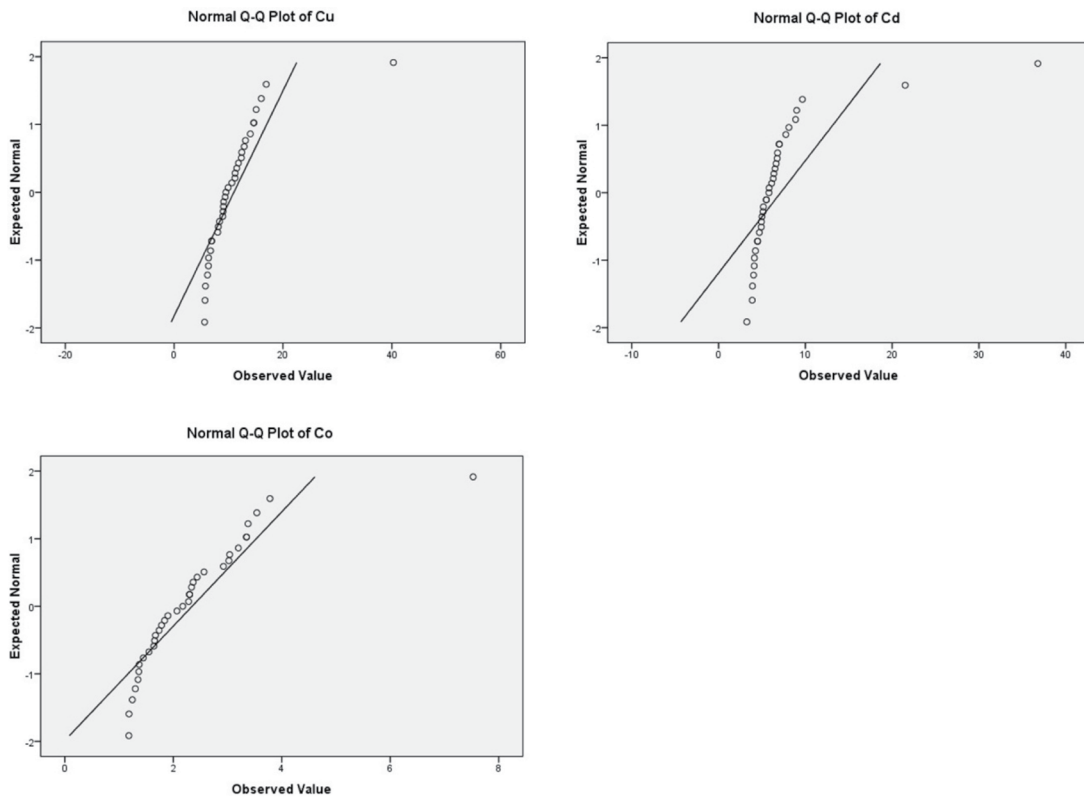


Fig. S1. Continued.